

Impacts of aviation fuel sulfur content on climate and human health

Zarashpe Z Kapadia^{1,2}, Dominick V. Spracklen², Steve R. Arnold², Duncan J. Borman³, Graham W. Mann^{2,4}, Kirsty J. Pringle², Sarah A. Monks^{2,*}, Carly L. Reddington², François Benduhn⁵, Alexandru Rap², Catherine E. Scott², Edward W. Butt², Masaru Yoshioka²

¹Doctoral Training Centre in Low Carbon Technologies, Energy Research Institute, School of Process Environmental and Materials Engineering, University of Leeds, Leeds, UK

²Institute for Climate and Atmospheric Science, School of Earth and Environment, University of Leeds, Leeds, UK

³Centre for Computational Fluid Dynamics, School of Civil Engineering, University of Leeds, Leeds, UK

⁴National Centre for Atmospheric Science, School of Earth and Environment, University of Leeds, Leeds, UK

⁵Institute for Advanced Sustainability Studies, Potsdam, Germany

*now at: Cooperative Institute for Research in Environmental Sciences, University of Colorado Boulder, Boulder, Colorado, USA

**now at: Chemical Sciences Division, NOAA Earth System Research Laboratory, Boulder, Colorado, USA

Abstract

Aviation emissions impact both air quality and climate. Using a coupled tropospheric chemistry-aerosol microphysics model we investigate the effects of varying aviation fuel sulfur content (FSC) on premature mortality from long-term exposure to aviation-sourced PM_{2.5} (particulate matter with a dry diameter of <2.5 µm) and on the global radiation budget due to changes in aerosol and tropospheric ozone. We estimate that present-day non-CO₂ aviation emissions with a typical FSC of 600 ppm result in ~3,600 [95% CI: 1,310–5,890] annual premature mortalities globally due to increases in cases of cardiopulmonary disease and lung cancer, resulting from increased surface PM_{2.5} concentrations. We quantify the global annual mean combined radiative effect (RE_{comb}) of non-CO₂ aviation emissions as –13.3 mW m⁻²; from increases in aerosols (direct radiative effect and cloud albedo effect) and tropospheric ozone.

Ultra-low sulfur jet fuel (ULSJ; FSC = 15 ppm) has been proposed as an option to reduce the adverse health impacts of aviation-induced PM_{2.5}. We calculate that swapping the global aviation fleet to ULSJ fuel would reduce the global aviation-induced mortality rate by ~620 [95% CI: 230–1020] mortalities a⁻¹ and increase RE_{comb} by +7.0 mW m⁻².

We explore the impact of varying aviation FSC between 0–6000 ppm. Increasing FSC increases aviation-induced mortality, while enhancing climate cooling through increasing the aerosol cloud albedo effect (CAE). We explore the relationship between the injection altitude of aviation emissions and the resulting climate and air quality impacts. Compared to the standard aviation emissions distribution, releasing aviation emissions at the ground increases global aviation-induced mortality and produces a net warming effect, primarily through a reduced CAE. Aviation emissions injected at the surface are 5 times less effective at forming cloud condensation nuclei, reducing the aviation-induced CAE by a factor of 10. Applying high FSCs at aviation cruise altitudes combined with ULSJ fuel at lower altitudes results in reduced aviation-induced mortality and increased negative RE compared to the baseline aviation scenario.

53 1 Introduction

54 Aviation is the fastest growing form of transport (Eyring et al., 2010; Lee et al., 2010; Uherek et al., 2010), with
55 a projected growth in passenger air traffic of 5% yr⁻¹ until 2030 (Barrett et al., 2012; ICAO, 2013), and a
56 projected near doubling of emissions by 2025, relative to 2005 (Eyers et al., 2004). These emissions, and
57 changes to them, have both climate and air quality impacts (Lee et al., 2009; Barrett et al., 2010; Woody et al.,
58 2011; Barrett et al., 2012).

59
60 Aviation emits a range of gas-phase and aerosol pollutants that can influence climate. Emissions of carbon
61 dioxide (CO₂) from aviation warm the climate (Lee et al., 2009; Lee et al., 2010). Emissions of nitrogen oxides
62 (NO_x) warm the climate through tropospheric ozone (O₃) formation, which acts as a greenhouse gas, and cool
63 climate via a decrease in the lifetime of the well-mixed greenhouse gas methane (CH₄) through increases in
64 the OH radical (Holmes et al., 2011; Myhre et al., 2011). Sulfate and nitrate aerosols, formed from aviation
65 sulfur dioxide (SO₂) and NO_x emissions and through altered atmospheric oxidants, lead to a cooling (Unger,
66 2011; Righi et al., 2013; Dessens et al., 2014), and black carbon (BC) emissions result in a warming (Balkanski
67 et al., 2010). Additionally, the formation of persistent linear contrails and contrail-cirrus from aircraft leads to
68 warming (Lee et al., 2010; Rap et al., 2010; Burkhardt and Karcher, 2011). Overall, aviation emissions are
69 thought to have a warming impact on climate, with net radiative forcing (RF) estimated as +55 mW m⁻²
70 (excluding cirrus cloud enhancement) (Lee et al., 2010).

71
72 Previous studies have separately assessed the impacts of aviation through different atmospheric species.
73 Short-term O₃ has been estimated to have a radiative effect ranging between 6–36.5 mW m⁻² (Sausen et al.,
74 2005; Köhler et al., 2008; Hoor et al., 2009; Lee et al., 2009; Holmes et al., 2011; Myhre et al., 2011; Unger,
75 2011; Frömming et al., 2012; Skowron et al., 2013; Unger et al., 2013; Khodayari et al., 2014; Brasseur et al.,
76 2015). The aerosol direct effect is highly uncertain [–28 to +20 mW m⁻²] (Righi et al., 2013), with the direct
77 aerosol effects for sulfate ranging between –0.9 to –7 mW m⁻² (Sausen et al., 2005; Fuglestad et al., 2008;
78 Lee et al., 2009; Balkanski et al., 2010; Unger, 2011; Gettelman and Chen, 2013; Brasseur et al., 2015), nitrate
79 ranging between –4 to –7 mW m⁻² (Unger et al., 2013; Brasseur et al., 2015), BC ranging between 0.1–0.3 mW
80 m⁻² (Sausen et al., 2005; Fuglestad et al., 2008; Lee et al., 2009; Balkanski et al., 2010; Unger, 2011;
81 Gettelman and Chen, 2013; Unger et al., 2013; Brasseur et al., 2015), and for organic carbon (OC) ranging
82 between –0.67 to –0.01 mW m⁻² (Sausen et al., 2005; Fuglestad et al., 2008; Lee et al., 2009; Balkanski et al.,
83 2010; Unger, 2011; Gettelman and Chen, 2013; Unger et al., 2013). Few studies estimate the aerosol cloud
84 albedo effect (aCAE) from aviation: Righi et al. (2013) assessed the aCAE to be –15.4±10.6 mW m⁻² while
85 Gettelman and Chen (2013) estimate –21±11 mW m⁻².

86
87 Aviation emissions can increase atmospheric concentrations of fine particulate matter with a dry diameter of
88 <2.5 µm (PM_{2.5}). Short-term exposure to PM_{2.5} can exacerbate existing respiratory and cardiovascular ailments,
89 while long-term exposure can result in chronic respiratory and cardiovascular diseases, lung cancer, chronic
90 changes in physiological functions and mortality (Pope et al., 2002; World Health Organisation, 2003; Ostro,
91 2004). In the U.S. aviation emissions are estimated to lead to adverse health effects in ~11,000 people (ranging
92 from mortality, respiratory ailments and hospital admissions due to exacerbated respiratory conditions) and
93 ~23,000 work loss days per annum (Ratliff et al., 2009). Landing and take-off aviation emissions increase PM_{2.5}
94 concentrations, particularly around airports (Woody et al., 2011), increasing US mortality rates by ~160 per
95 annum.

96
97 Previous studies have estimated the number of premature mortalities due to exposure to pollution resulting
98 from aviation emissions. Barrett et al. (2012) and Barrett et al. (2010) used the methodology of Ostro (2004)
99 to estimate that aviation emissions are responsible for ~10,000 premature mortalities a⁻¹ due increases in
100 cases of cardiopulmonary disease and lung cancer. Yim et al. (2015) using the same methodology but with the
101 inclusion of the Rapid Dispersion Code (RDC) to simulate the local air quality impacts of aircraft ground level
102 emissions estimated 13,920 (95% CI: 7,220–20,880) mortalities a⁻¹. Morita et al. (2014) using the integrated
103 exposure–response (IER) model from Burnett et al. (2014) to derive relative risk (RR) estimate that aviation
104 results in 405 (95% CI: 182–648) mortalities a⁻¹ due to increases in cases of lung cancer, stroke, ischemic heart
105 disease, trachea, bronchus, and chronic obstructive pulmonary disease. Jacobson et al. (2013) estimate 310

(95% CI: -400 to 4,300) mortalities a⁻¹ from aviation emissions due to cardiovascular effects. Taking these studies in account, the different methodologies applied and modes of mortality investigated aviation is estimated to be responsible for between 310–13,920 mortalities a⁻¹.

The introduction of cleaner fuels and pollution control technologies can improve ambient air quality and reduce adverse health effects of fossil fuel combustion (World Health Organisation, 2005). One proposed solution to reduce the adverse health effects of aviation-induced PM_{2.5} is the use of ultra-low sulfur jet fuel (ULSJ), reducing the formation of sulfate aerosol (Barrett et al., 2012; Barrett et al., 2010; Ratliff et al., 2009; Hileman and Stratton, 2014). ULSJ fuels typically have a fuel sulfur content (FSC) of 15 ppm, compared with an FSC of between 550–750 ppm in standard aviation fuels (Barrett et al., 2012). The current global regulatory standard for aviation fuel is a maximum FSC of 3000 ppm (Ministry of Defence, 2011; ASTM International, 2012).

Despite the potential for decreased emission of SO₂, application of ULSJ fuel will not completely remove the impacts of aviation on PM_{2.5}. It is estimated that over a half of aviation-attributable surface-level sulfate is associated with oxidation of non-aviation SO₂ by OH produced from aviation NO_x emissions, and not directly produced from aviation-emitted SO₂ (Barrett et al., 2010). Therefore, even a completely desulfurised global aviation fleet would likely contribute a net source of sulfate PM_{2.5}. Nevertheless, previous work has shown that the use of ULSJ fuel reduces global aviation-induced PM_{2.5} by ~23%, annually avoiding ~2300 (95% CI: 890–4200) mortalities (Barrett et al., 2012).

Altering the sulfur content of aviation fuel also modifies the net climate impact of aviation emissions. A reduction in fuel sulfur content reduces the formation of cooling sulfate aerosols (Unger, 2011; Barrett et al., 2012), increasing the net warming effect of aviation emissions. The roles of sulfate both in climate cooling and in increasing surface PM_{2.5} concentrations mean that policy makers must consider both health and climate when considering effects from potential reductions in sulfur emissions from a given emissions sector (Fiore et al., 2012).

In this study, we investigate the impacts of changes in the sulfur content of aviation fuel on climate and human health. A coupled tropospheric chemistry-aerosol microphysics model is used to quantify global atmospheric responses in aerosol and O₃ to varying FSC scenarios. Radiative effects due to changes in tropospheric O₃ and aerosols are calculated using a radiative transfer model the impacts of changes in surface PM_{2.5} on human health are estimated using concentration response functions. Using a coupled tropospheric chemistry-aerosol microphysics model that includes nitrate aerosol allows us to assess the impacts of nitrate and aerosol indirect effects in addition to the ozone and aerosol direct effects that have been more routinely calculated.

2 Methods

2.1 Coupled chemistry-aerosol microphysics model

2.1.1 Model description

We use GLOMAP-mode (Mann et al., 2010), embedded within the 3-D off-line Eulerian chemical transport model TOMCAT (Arnold et al., 2005; Chipperfield, 2006). Meteorology (wind, temperature and humidity) and large scale transport is specified from interpolation of 6-hourly European Centre for Medium Range Weather Forecasts (ECMWF) reanalysis (ERA-40) fields (Chipperfield, 2006; Mann et al., 2010). Cloud fraction and cloud top pressure fields are taken from the International Satellite Cloud Climatology Project (ISCCP-D2) archive for the year 2000 (Rossow and Schiffer, 1999).

GLOMAP-mode is a two-moment aerosol microphysics scheme representing particles as an external mixture of 7 size modes (4 soluble and 3 insoluble) (Mann et al., 2010). We use the nitrate-extended version of GLOMAP-mode (Benduhn et al., 2016) which, as well as tracking size-resolved sulfate, BC, OC, sea-salt and dust components, also includes a dissolution solver to accurately characterise the size-resolved partitioning of

ammonia and nitric acid into ammonium and nitrate components in each soluble mode. Aerosol components are assumed to be internally mixed within each mode. GLOMAP-mode includes representations of nucleation, particle growth via coagulation, condensation and cloud processing, wet and dry deposition, and in- and below-cloud scavenging (Mann et al., 2010).

TOMCAT includes a tropospheric gas-phase chemistry scheme (inclusive of O_x - NO_y - HO_x), treating the degradation of C_1 - C_3 non-methane hydrocarbons (NMHCs) and isoprene, together with a sulfur chemistry scheme (Spracklen et al., 2005; Breider et al., 2010; Mann et al., 2010). The tropospheric chemistry is coupled to aerosol as described in Breider et al. (2010).

The nitrate-extended version of the TOMCAT-GLOMAP-mode coupled model used in this investigation employs a hybrid solver to simulate the dissolution of semi-volatile inorganic gases (such as H_2O , HNO_3 , HCl and NH_3) into the aerosol-liquid-phase.

Emissions of DMS are calculated using monthly mean sea-water concentrations of DMS from (Kettle and Andreae, 2000), driven by ECMWF winds and sea-air exchange parameterisations from Nightingale et al. (2000). Emissions of SO_2 are included from both continuous (Andres and Kasgnoc, 1998) and explosive volcanoes (Halmer et al., 2002), and wildfires for year 2000 (Van Der Werf et al., 2003; Dentener et al., 2006). Anthropogenic SO_2 emissions (including industrial, power-plant, road-transport, off-road-transport and shipping sectors) are representative of the year 2000 (Cofala et al., 2005). Emissions of monoterpenes and isoprene are from Guenther et al. (1995). NH_3 emissions are from the EDGAR inventory (Bouwman et al., 1997). NO_x emissions are considered from anthropogenic (Lamarque et al., 2010), natural (Lamarque et al., 2005) and biomass burning (van der Werf et al., 2010) sources.

Annual mean emissions of BC and OC aerosol from fossil fuel and biofuel combustion are from Bond et al. (2004). Monthly wildfire emissions are taken from the GFED v1 (Global Fire Emissions Database) for the year 2000 (Van Der Werf et al., 2003). For primary aerosol emissions we use geometric mean diameters (D_g) with standard deviations as described by Mann et al. (2010).

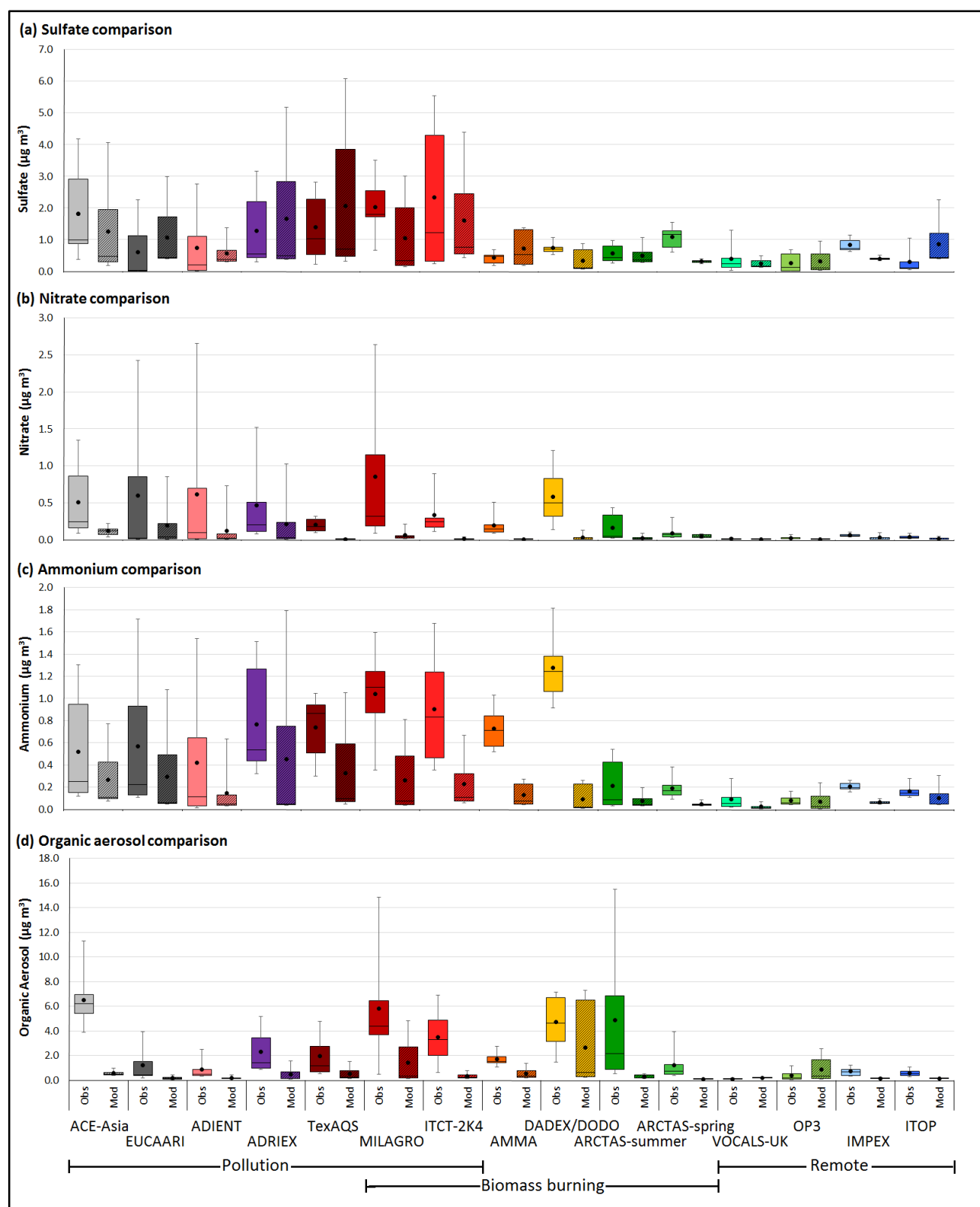
Here, we ran simulations at a horizontal resolution of $2.8^\circ \times 2.8^\circ$ with 31 hybrid σ -p levels extending from the surface to 10 hPa. All simulations were conducted for 16 months from September 1999 to December 2000 inclusive, with the first four months discarded as spin-up time.

2.1.2 Model evaluation

GLOMAP has been extensively evaluated against observations including comparisons of speciated aerosol mass (Mann et al., 2010; Spracklen et al., 2011b), aerosol number (Mann et al., 2010; Spracklen et al., 2010) and cloud condensation nuclei (CCN) concentrations (Spracklen et al., 2011a). TOMCAT simulated fields have been evaluated against observations, with CO and O_3 evaluated against aircraft observations (Arnold et al., 2005), Mediterranean summertime ozone against satellite observations (Richards et al., 2013), along with O_3 evaluated against satellite observations (Chipperfield et al., 2015). Benduhn et al. (2016) shows that simulated surface concentrations of NO_3 and NH_4 are in reasonable agreement with observations in Europe, the U.S. and East Asia. Here we focus our evaluation on the aerosol vertical profile and as well as nitrate aerosol which has not been evaluated previously.

Fig. 1 presents simulated sulfate, nitrate, ammonium and organic aerosol mass concentrations in comparison to airborne observations compiled by Heald et al. (2011). Observations were predominantly made using an Aerodyne Aerosol Mass Spectrometer (AMS). Simulated profiles are for year 2000, while observational aerosol profiles are from field campaigns conducted between 2001 and 2008.

210 **Fig. 1: Comparison of observed (Obs) and simulated (Mod) (a) sulfate; (b) nitrate; (c) ammonium, and; (d)**
 211 **organic aerosol mass concentrations. Observations are from airborne field campaigns compiled by Heald et**
 212 **al. (2011). Mean values are represented by black dots, median values as shown by horizontal lines, while**
 213 **boxes denote the 25th and 75th percentiles, and whiskers denote the 5th and 95th percentile values.**



214 Overall we find the model overestimates sulfates [NMB = +16.9%], while underestimating nitrates [NMB = –
 215 60.7%], ammonium [NMB = –47.1%] and organic aerosols (OA) [NMB = –56.2%]. Model skill varies dependant
 216 on the conditions affecting each field campaign. To explore this, we use the broad stratification of the field
 217 campaigns into anthropogenic pollution, biomass burning and remote conditions as used by Heald et al. (2011)

and shown in Fig. 1. The model underestimates aerosol concentrations in biomass burning regions [sulfate NMB = -14.9%; nitrate NMB = -79.4%; ammonium NMB = -68.7%, and; OA NMB = -74.5%]. These model underestimations could partly due to very concentrated plumes in these regions affecting campaign mean concentrations. The model performs better in polluted [sulfate NMB = +31.6%; nitrate NMB = -56.2%; ammonium NMB = -28.6%, and; OA NMB = -40.9%], and remote regions [sulfate NMB = +25.4%; nitrate NMB = -6.4%; ammonium NMB = -20.2%, and; OA NMB = -41.5%].

The overestimation of sulfate aerosol is likely due to the decline in anthropogenic SO₂ emissions in Europe and the US between 2000–2008 (Vestreng et al., 2007; Hand et al., 2012). An underestimation of OA has been reported previously (Heald et al., 2011; Spracklen et al., 2011b) and is likely due to an underestimate in SOA formation in the model. Whitburn et al. (2015) found biomass burning emissions of NH₃ may be underestimated which would affect a number of our comparisons.

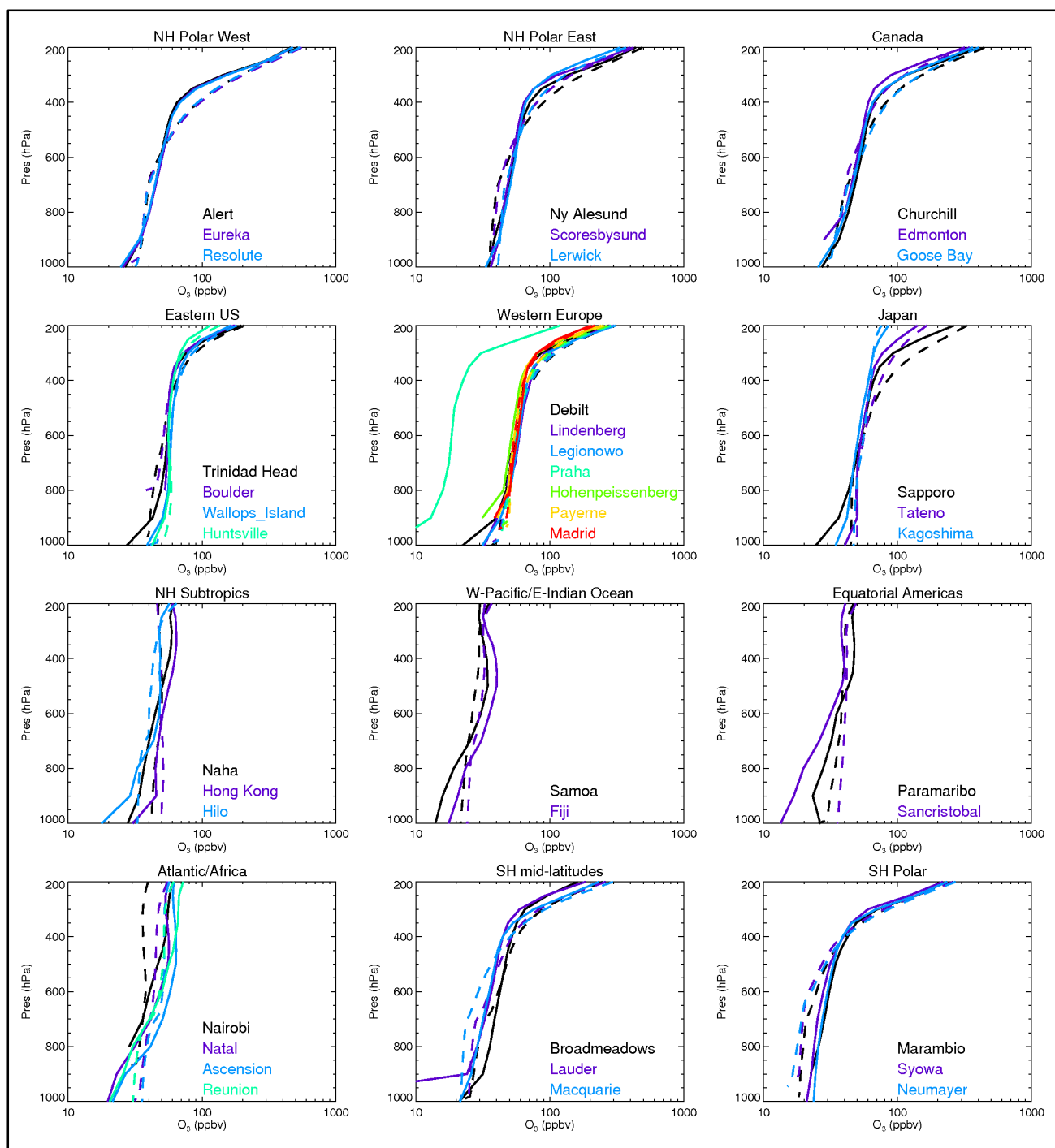
Fig. 2 presents simulated ozone concentration profiles in comparison to ozonesonde observations compiled by Tilmes et al. (2012). Observations were compiled from three networks, comprising of 41 stations with continuous sampling from 1995 to 2011: (i) The World Ozone and Ultraviolet Data Center (WOUDC) (<http://www.woudc.org/>); (ii) the Global Monitoring Division (GMD, <ftp://ftp.cmdl.noaa.gov/ozwv/ozone/>), and (iii) The Southern Hemisphere Additional OZonesondes (SHADOZ) (Tilmes et al., 2012).

Regional model-observation comparison profiles presented in Fig. 2 demonstrate good agreement between the model and ozonesonde profiles, while demonstrating regional variations driven by variations in tropopause height, showing no evidence of systematic model bias in the upper troposphere. Notable differences are seen between simulated and observed ozone profiles over the Praha launch site in Western Europe, with the model greatly overestimating observed ozone.

Evaluation of ozone model bias is conducted for the troposphere, using a chemical tropopause definition of 150 ppbv ozone, as previously used by Stevenson et al. (2013), Young et al. (2013) and Rap et al. (2015). We find the model overestimates global ozone concentrations [NMB = +7.0%] with overestimates in Western Europe [+18.9%] and the Northern Hemisphere Polar West [NMB = +14.4%] regions and underestimates over the Atlantic/Africa [NMB = -11.0%] and Southern Hemisphere Polar [NMB = -4.6%] regions.

Differences between model and observational profiles can in part be explained by the differences in years of simulation and observation, a poor representation of deep convection resulting in model underestimations in the tropics and overestimations downwind (Thompson et al., 1997), in tandem with reductions in anthropogenic NO_x emissions over this time period (Konovalov et al., 2008).

272 **Fig. 2: Comparison of observed (solid lines) and simulated (dashed lines) ozone profiles. Observations are**
 273 **taken from ozonesonde observations, and arranged by launch location regions according to Tilmes et al.**
 274 **(2012).**



275
 276
 277
 278
 279
 280
 281
 282
 283
 284

285 2.2 Aviation emissions

286 Aircraft emit NO_x, carbon monoxide (CO), SO₂, BC, OC and hydrocarbons (HCs). The historical emissions dataset
 287 for the CMIP5 (5th Coupled Model Intercomparison Project) model simulations used by the IPCC 5th Assessment
 288 Report only included NO_x and BC aviation emissions (Lamarque et al., 2009). Recently there have been efforts
 289 to add HCs, CO and SO₂ emissions to aviation emission inventories (Eyers et al., 2004; Quantify Integrated
 290 Project, 2005-2012; Wilkerson et al., 2010).

291
 292 Here we develop a new 3-D civil aviation emissions dataset for the year 2000, based on CMIP5 historical
 293 aviation emissions (Lamarque et al., 2009). The new dataset includes emissions of NO_x, CO, SO₂, BC, OC, and
 294 HCs. In contrast to existing datasets which provide a general emissions index for HCs (Eyers et al., 2004) we
 295 speciate HCs as formaldehyde (HCHO), ethane (C₂H₆), propane (C₃H₈), methanol (CH₃OH), acetaldehyde
 296 (CH₃CHO), and acetone ((CH₃)₂CO).

297
 298 Table 1 describes our new emissions dataset. NO_x and BC emissions are taken directly from Lamarque et al.
 299 (2009). We calculate fuelburn from BC emissions data and the BC emissions index (Eyers et al., 2004) as used
 300 by Lamarque et al. (2009). Following DuBois and Paynter (2006), we assume that BC emissions scale linearly
 301 with fuel consumption. We estimate emissions for other species using our calculated aviation fuelburn in
 302 combination with published species-specific emissions indices (EI reported in g kg⁻¹ of fuel). Emission indices
 303 for CO and SO₂ are from the FAA's aviation environmental design tool (AEDT) (Wilkerson et al., 2010). OC
 304 emissions are calculated using a BC:OC ratio of 4 (Hopke, 1985; Bond et al., 2004); resulting in an EI within the
 305 range determined by Wayson et al. (2009). Speciated hydrocarbon emissions are calculated from experimental
 306 data following the methodology of Wilkerson et al. (2010) using experimental data from Knighton et al. (2007)
 307 and Anderson et al. (2006), in conjunction with operating parameters suggested by the Airbus Flight Crew
 308 Training manual (Airbus, 2008).

309
 310 **Table 1: Aviation emissions indices and total annual emissions for year 2000**
 311

| Species | Emissions index (g kg ⁻¹ of fuel) | Global emissions for year 2000 (Tg of species) | Range of annual global emissions from previous studies (Tg of species) |
|------------------------------------|---|---|--|
| NO _x | 13.89 ^a | 2.786 | 1.98–3.286 ^{a,b,j,i,k,l} |
| CO | 3.61 ^b | 0.724 | 0.507–0.679 ^{b,h,i,j} |
| HCHO | 1.24 ^{c,d} | 0.249 | 0.01205 ^b |
| C ₂ H ₆ | 0.0394 ^e | 0.007899 | 0.00051 ^b |
| C ₃ H ₈ | 0.03 ^e | 0.006014 | 0.00444 ^b |
| CH ₃ OH | 0.22 ^d | 0.044 | 0.00177 ^b |
| CH ₃ CHO | 0.33 ^d | 0.066 | 0.00418 ^b |
| (CH ₃) ₂ CO | 0.18 ^d | 0.036 | 0.00036 ^b |
| SO ₂ | 1.1760 ^b | 0.236 | 0.182–0.221 ^{a,b,h,i,j} |
| BC | 0.0250 ^a | 0.005012 | 0.0039–0.0068 ^{a,b,h,i,j,k} |
| OC | 0.00625 ^{f,g} | 0.001253 | 0.003 ^{b,i} |

^a(Eyers et al., 2004), ^b(Wilkerson et al., 2010), ^c(Spicer et al., 1994), ^d(Knighton et al., 2007),
^e(Anderson et al., 2006), ^f(Bond et al., 2004), ^g(Hopke, 1985), ^h(Olsen et al., 2013), ⁱ(Unger, 2011),
^j(Lee et al., 2010), ^k(Lamarque et al., 2010), ^l(Quantify Integrated Project, 2005-2012)

312
 313 Our global aviation emissions typically lie within the range of previous studies (Table 1). Our SO₂ emissions are
 314 greater than those used by Wilkerson et al. (2010) for 2006, despite the use of the same EI. This is due to the
 315 greater global fuelburn considered by the base inventory used to develop our emissions inventory (Eyers et
 316 al., 2004; Lamarque et al., 2010). Our estimated OC emissions are lower than the emissions estimated in the
 317 AEDT 2006 inventory, due to the lower EI applied here. The lower EI_{OC} applied here (in comparison to
 318 Wilkerson et al. (2010)) is a due to the phase of flight considered when deriving the AEDT emissions inventory;
 319 where they derive EI_{OC} focusing on airport operations at ground level condition acknowledging the risk of

overestimating aviation OC emissions, while in comparison we consider aircraft operations after ground idle conditions which risks underestimating aviation OC emissions.

We calculate the geometric mean diameter (D_g) for internally mixed BC/OC particles as 50.5 nm from the mean particle mass derived using the particle number emissions index (Eyers et al., 2004) and a constant standard deviation set to $\sigma = 1.59$ nm.

2.3 Fuel sulfur content simulations

To explore the impact of aviation FSC on climate and air quality we performed a series of 11 global model experiments (Table 2). In 7 of these model experiments FSC values were varied globally between zero and 6000 ppm. Three further simulations varied the vertical distribution of aviation emissions. The first simulation collapses all aviation emissions to ground level (GROUND), in order to compare an equivalent ground emission source and its effects. Two simulations (SWITCH1 and SWITCH2), use a low FSC (15 ppm) applied below the cruise phase of flight (<8.54 km altitude) (Lee et al., 2009; Köhler et al., 2013) combined with a high FSC at altitudes above. The SWITCH1 scenario increases FSC in line with our HIGH scenario above 8.54 km, while in the SWITCH2 scenario, emissions are scaled such that total global sulfur emissions are the same as the standard simulation (NORM), resulting in a FSC of 1420 ppm above 8.54 km. Results from all simulations are compared against a simulation with aviation emissions excluded (NOAVI).

Table 2: FSC and global SO₂ emissions applied in each model experiment.

| Scenario name | Description | FSC (ppm) | Total SO ₂ emitted (Tg) |
|---------------|--|-----------|------------------------------------|
| NOAVI | No aviation emissions | n/a | 0.0 |
| NORM | Standard aviation emissions scenario | 600 | 0.236 |
| DESUL | Desulfurised case | 0 | 0.0 |
| ULSJ | Ultra low sulfur jet fuel | 15 | 0.006 |
| HALF | Half FSC of normal case | 300 | 0.118 |
| TWICE | Twice FSC of normal case | 1200 | 0.472 |
| HIGH | FSC at international specification limit | 3000 | 1.179 |
| OVER | Twice FSC specification limit | 6000 | 2.358 |
| GROUND | All emissions emitted at surface level (FSC as NORM) | 600 | 0.236 |
| SWITCH1 | ULSJ FSC to 8.54 km, HIGH FSC content above | 15/3000 | 0.491 |
| SWITCH2 | ULSJ FSC to 8.54 km, FSC = 1420 ppm above | 15/1420 | 0.236 |

2.4 Radiative impacts

We calculate the aerosol direct radiative effect (aDRE), aerosol cloud albedo effect (aCAE) and tropospheric O₃ direct radiative effect (O3DRE) using the offline Edwards and Slingo (1996) radiative transfer model. The radiative transfer model considers 6 bands in the shortwave (SW) and 9 bands in the longwave (LW), adopting a delta-Eddington 2 stream scattering solver at all wavelengths. The top-of-the-atmosphere (TOA) aerosol aDRE and aCAE are calculated using the methodology described in Rap et al. (2013) and Spracklen et al. (2011a), with the method for O3DRE as in Richards et al. (2013). To determine the aCAE we calculated cloud droplet number concentrations (CDNCs) using the monthly mean aerosol size distribution simulated by GLOMAP combined with parameterisations from Nenes and Seinfeld (2003), updated by Fountoukis and Nenes (2005) and Barahona et al. (2010). CDNC were calculated with a prescribed updraft velocity of 0.15 m s⁻¹ over ocean and 0.3 m s⁻¹ over land. Changes to CDNC were then used to perturb the effective radii of cloud droplets in low- and mid-level clouds (up to 600 hPa). The aDRE, aCAE and O3DREs for each aviation emissions scenario are calculated as the difference in TOA net (SW + LW) radiative flux compared to the NOAVI simulation.

2.5 Health effects

We calculate excess premature mortality from cardiopulmonary diseases and increases in cases of lung cancer due to long-term exposure to aviation-induced PM_{2.5} (Ostro, 2004). Using this function allows us to compare directly with previous studies (Barrett et al., 2012; Yim et al., 2015); in future work estimates are required with updated methodologies (Burnett et al., 2014). PM_{2.5} is used as a measure of likely health impacts because chronic exposure is associated with adverse human health impacts including morbidity and mortality (Dockery et al., 1993; Pope and Dockery, 2006).

We relate annual excess mortality to annual mean surface PM_{2.5} via a concentration response-function (CRF) (Ostro, 2004). This response-function considers concentrations of PM_{2.5} for a perturbed case (X) (defined by aviation emissions scenarios from Table 2) in relation to a baseline case with no aviation emissions (X₀) (NOAVI). To calculate excess mortality, the relative risk (RR) for both cardiopulmonary disease and lung cancer are calculated according to Ostro (2004) using a function of baseline (X₀) and perturbed (X) PM_{2.5} concentrations, and the disease specific cause-specific coefficient (β):

$$RR = \left[\frac{(X+1)}{(X_0+1)} \right]^\beta \quad (1)$$

β coefficients for cardiopulmonary disease mortality of 0.15515 [95% CI = 0.05624–0.2541] and lung cancer of 0.232 [95% CI = 0.086–0.379] are used (Pope et al., 2002; Ostro, 2004). The 95% confidence interval (CI) in β allow low-, mid- and high-range mortality values to be calculated. The attribution factor (AF) from the exposure to air pollution is calculated using equation (2):

$$AF = (RR - 1)/RR \quad (2)$$

Excess mortality (E) for both cardiopulmonary disease and lung cancer are calculated using baseline mortality rates (B), the fraction of the population over 30 years old (P₃₀), along with the AF:

$$E = AF \times B \times P_{30} \quad (3)$$

Global population data is taken from the Gridded World Population (GWP; version3) project (Center for International Earth Science Information Network, 2012) with country specific data on the fraction of the population under 30.

3 Results

3.1 Surface PM_{2.5}

Fig. 3 shows the simulated impact of aviation emissions with standard FSC (FSC = 600 ppm; NORM) on surface PM_{2.5} concentrations. Aviation increases annual mean PM_{2.5} concentrations by up to ~80 ng m⁻³ (relative to the NOAVI simulation) over Central Europe and Eastern China (Fig. 3(a)). Aviation emissions result in largest fractional changes in annual mean PM_{2.5} concentrations (up to 0.8%) over North America and Europe (Fig. 3(b)).

Fig. 3: Impact of aviation emissions (FSC = 600 ppm) on surface annual mean PM_{2.5} concentrations. (a) absolute (NORM–NOAVI) and (b) percentage changes. Boxes show the European (20°–40°E, 35°N–66°N) and North American (146°W–56°W, 29°N–72°N) regions.

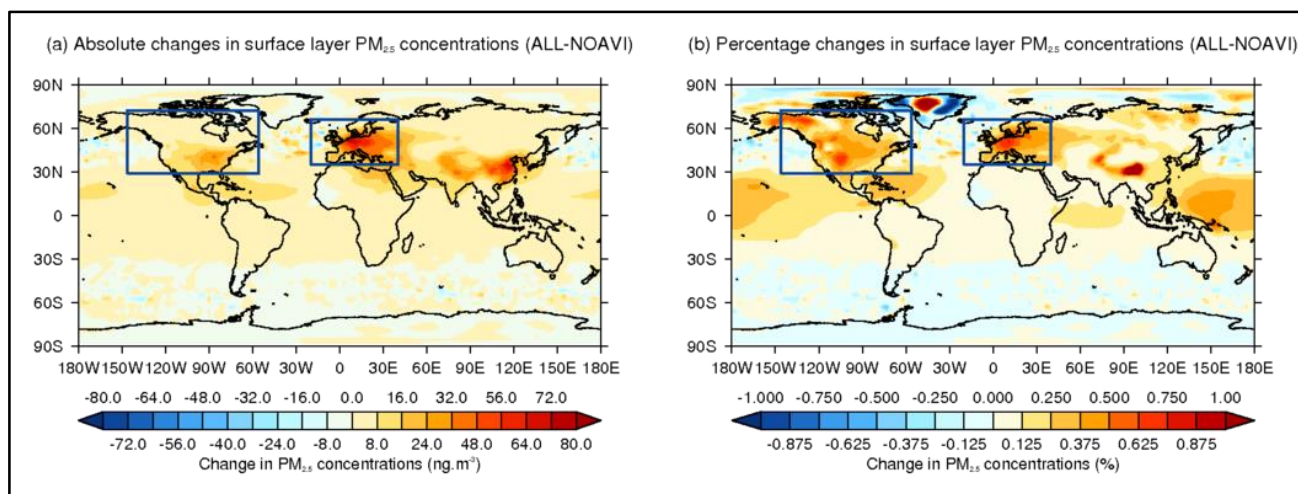


Fig. 4 shows the impact of aviation emissions on global and regional mean PM_{2.5} concentrations, as a function of FSC. With standard FSC (FSC = 600 ppm), aviation increases global mean surface PM_{2.5} concentrations by 3.9 ng m⁻³; with increases in PM_{2.5} dominated by sulfates [56.2%], nitrates [26.0%] and ammonium [16.0%]. Aviation emissions increase European annual mean PM_{2.5} concentrations by 20.3 ng m⁻³ (Fig. 4(b)), substantially more than over North America (Fig. 4(c)) where an annual mean increase of 6.3 ng m⁻³ is simulated. Increased PM_{2.5} is dominated by nitrates, both over Europe [55.5%] and over North America [44.4%]. Sulfates contribute up to 44.6% of increases in PM_{2.5} over North America, and 30.0% over Europe.

The use of ULSJ fuel (FSC = 15 ppm) reduces global annual mean surface aviation-induced PM_{2.5} concentrations (in relation to the NORM case) by 35.7% [1.4 ng m⁻³] (Fig. 4); predominantly due to changes in sulfate [-1.4 ng m⁻³; -62.1%] and ammonium [-0.2 ng m⁻³; -37.9%], which are marginally offset by very small increases in nitrates [+3.2x10⁻³ ng m⁻³; +0.3%]. Aviation emissions also leads to small changes to other aerosol components of +0.2 ng; which includes natural aerosols such as dust [+0.3 ng m⁻³; +61.8%], sodium [-19.5%] and chloride from sea-salt [-19.5%] with the changes due to changes in aerosol lifetimes, along with changes in BC [-7.9%] and OC [-19.3%].

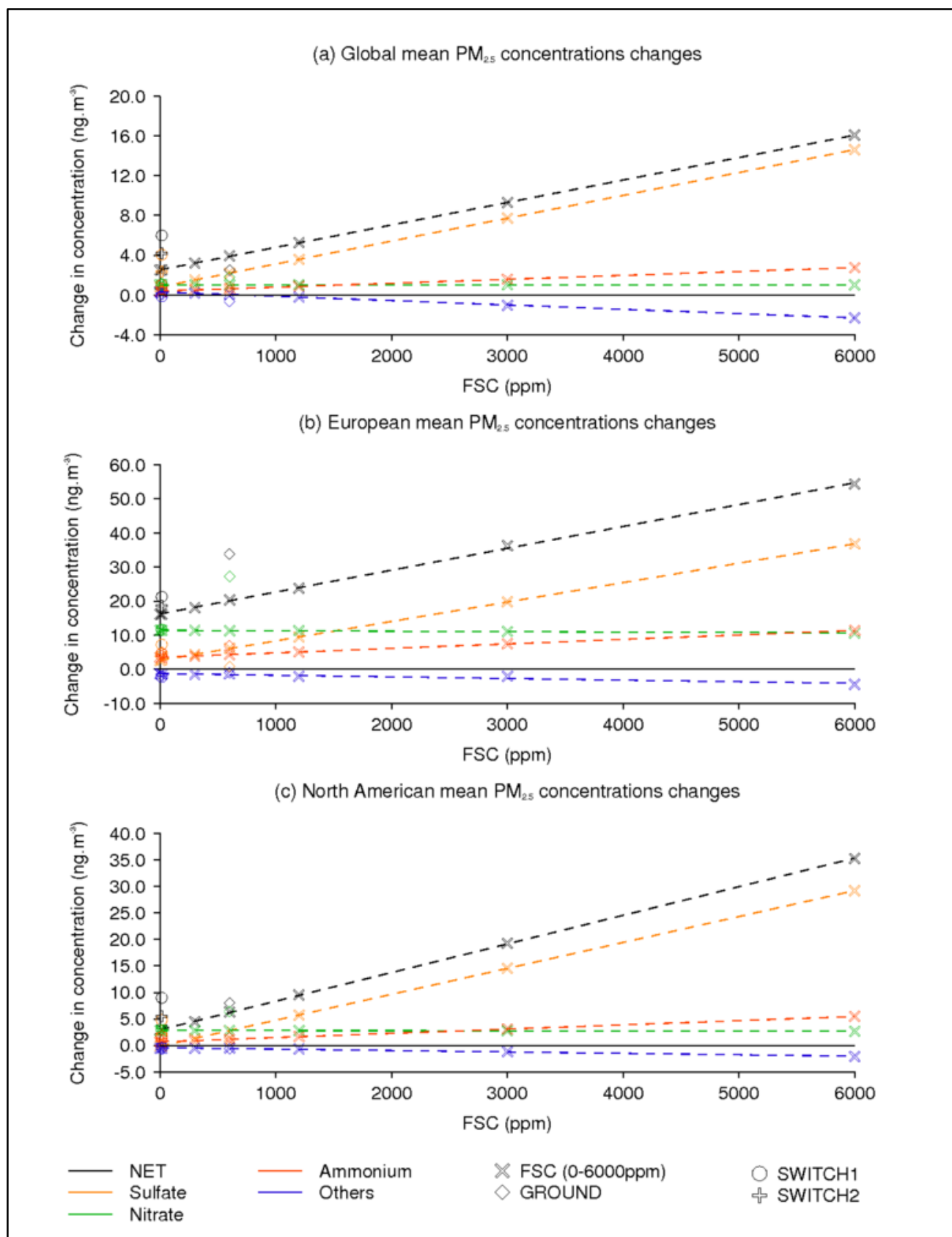
In comparison to the global mean, switching to the use of ULSJ fuel in aviation larger absolute reductions in PM_{2.5} of -4.2 ng m⁻³ are simulated over Europe [Δ sulfate = -3.4 ng m⁻³; Δ nitrate = +0.1 ng m⁻³; Δ ammonium = -0.8 ng m⁻³; and Δ others = -0.1 ng m⁻³] and of -3.4 ng m⁻³ over North America [Δ sulfate = -2.9 ng m⁻³; Δ nitrate = +0.02 ng m⁻³; Δ ammonium = -0.5 ng m⁻³; and Δ others = -0.01 ng m⁻³] (Fig. 4 (b,c)). Over North America, swapping to ULSJ fuel reduces aviation-induced PM_{2.5} by 53.4%, while a smaller reduction of 20.5% is simulated over Europe. The smaller fractional change in PM_{2.5} over Europe is caused by smaller reductions in aviation-induced sulfate [-55.9%] and ammonium [-18.4%] compared to over North America, which sees a reduction in ammonium of 41.6% and a reduction in sulfates of 103% indicating that over the US the ULSJ fuel scenario sees a reduction in sulfates in relation to a NOAVI scenario.

Complete desulfurisation of jet fuel (FSC = 0 ppm; DESUL) reduces global mean aviation-induced surface PM_{2.5} concentrations by 36.5% [-1.43 ng m⁻³], with changes in sulfates [-1.40 ng m⁻³; -63.5%] and ammonium [-0.24 ng m⁻³; -38.8%] dominating. Under this scenario the reductions in surface sulfate PM_{2.5} from aviation are 57.3% over Europe and 105% over North America. ULSJ fuel therefore gives similar results to complete desulfurisation, due to the very small sulfur emission from ULSJ fuel (Table 2).

In summary, increases in FSC result in increased surface PM_{2.5}, due to increased sulfate outweighing the small reductions in nitrate. Simulated changes in sulfate, nitrate, ammonium and total PM_{2.5} are linear ($R^2 > 0.99$, p -value < 0.001 globally and for all individual regions) with respect to FSC (Fig. 4). Larger emission perturbations would likely lead to a non-linear response in atmospheric aerosol. The impact of variations in FSC on PM_{2.5} are

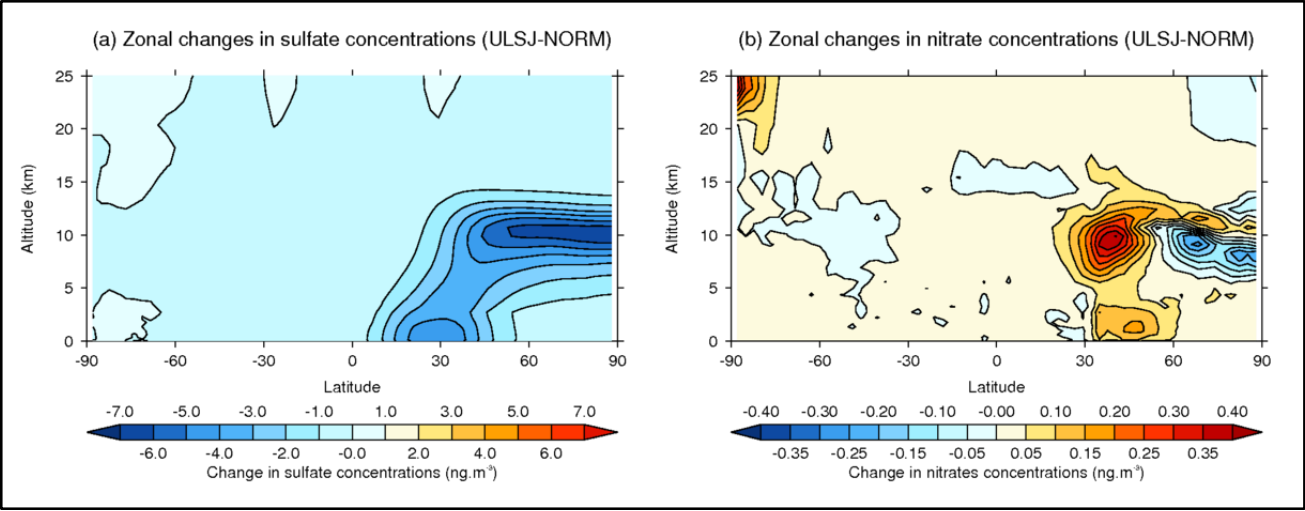
regionally variable; over Europe changes in $PM_{2.5}$ concentrations are observed to be more sensitive to changes in FSC than over North America, and the global domain.

Fig. 4: Impact of aviation FSC on (a) global, (b) European (20°–40°E, 35°N–66°N), (c) North American (146°W–56°W, 29°N–72°N) surface annual mean $PM_{2.5}$ mass concentrations: FSC variations (×), GROUND (◇), SWITCH1 (–), and SWITCH2 (+) simulations. Solid lines demonstrate the linear relationship between FSC and $PM_{2.5}$.



451

452 **Fig. 5: Simulated differences in zonal annual mean sulfate (a) and nitrate (b) concentrations from the use of**
453 **ULSJ fuel relative to standard fuel (ULSJ–NORM).**



454

455 Fig. 5 shows the impact of changing to ULSJ fuel on zonal mean sulfate and nitrate concentrations relative to
456 standard fuel (NORM). Table 3 reports the global aerosol burden from aviation under different emission
457 scenarios. With standard FSC (FSC = 600 ppm), the global aviation-induced aerosol burden is 16.9 Gg,
458 dominated by sulfates (76.3%) and nitrates (33.4%). The use of ULSJ (FSC = 15 ppm) reduces the global aerosol
459 burden from aviation by 26.8%. Complete desulfurisation of aviation fuel reduces the global aerosol burden
460 from aviation by 28.4%, with the global sulfate burden from aviation reduced by 71.6% (Table 3). When
461 aviation emissions contain no sulfur, aviation-induced sulfate is formed through aviation NO_x-induced
462 increases in OH concentrations, resulting in the oxidation of SO₂ from non-aviation sources (Unger et al., 2006;
463 Barrett et al., 2010).

464

465 **Table 3: Global aviation-induced aerosol mass burdens for different emission scenarios. Values in**
466 **parentheses show percentage change relative to NORM case.**

| Scenario | All components (Gg) | Sulfates (Gg) | Nitrates (Gg) |
|--|------------------------|------------------|------------------|
| NORM | 16.9 | 12.9 | 5.7 |
| ULSJ | 12.4 (–26.8%) | 4.0 (–69.1%) | 5.9 (+4.5%) |
| DESUL | 12.1 (–28.4%) | 3.7 (–71.6%) | 6.0 (+5.1%) |
| No NO _x and SO ₂ | 2.0 (–88.3%) | 0.3 (–97.5%) | 0.1 (–97.9%) |

467

468 In line with previous work, we find a substantial fraction of aviation sulfate can be attributed to aviation NO_x
469 emissions and not directly to aviation SO₂ emissions. We estimate that 36% aviation-attributable sulfates
470 formed at the surface are associated with aviation NO_x emissions, compared to ~63% estimated by Barrett et
471 al. (2010) using the GEOS-Chem model (both estimates for FSC = 600 ppm). Differences between model
472 estimates can be attributed to differences in model chemistry and microphysics, and different aviation NO_x
473 emissions. We find desulfurisation increases the aviation nitrate burden by 5.1% (Table 3); although much of
474 this increase occurs at altitudes well above the surface (Fig. 5) and so is not reflected in surface PM_{2.5}
475 concentrations.

476

477 We explored the impacts of NO_x emission reductions in combination with fuel desulfurisation. A scenario with
478 desulfurised fuel and zero NO_x emissions reduces the global aviation-induced aerosol burden by 88.3% (Table
479 3), in comparison to a desulfurised only case (DESUL), where the aviation-induced aerosol burden is reduced
480 by 28.4%. Removal of aviation NO_x and SO₂ emissions results in a 95.0% reduction in aviation-induced global
481 mean surface level aviation-induced PM_{2.5}. These results imply that only limited sulfate reductions can be

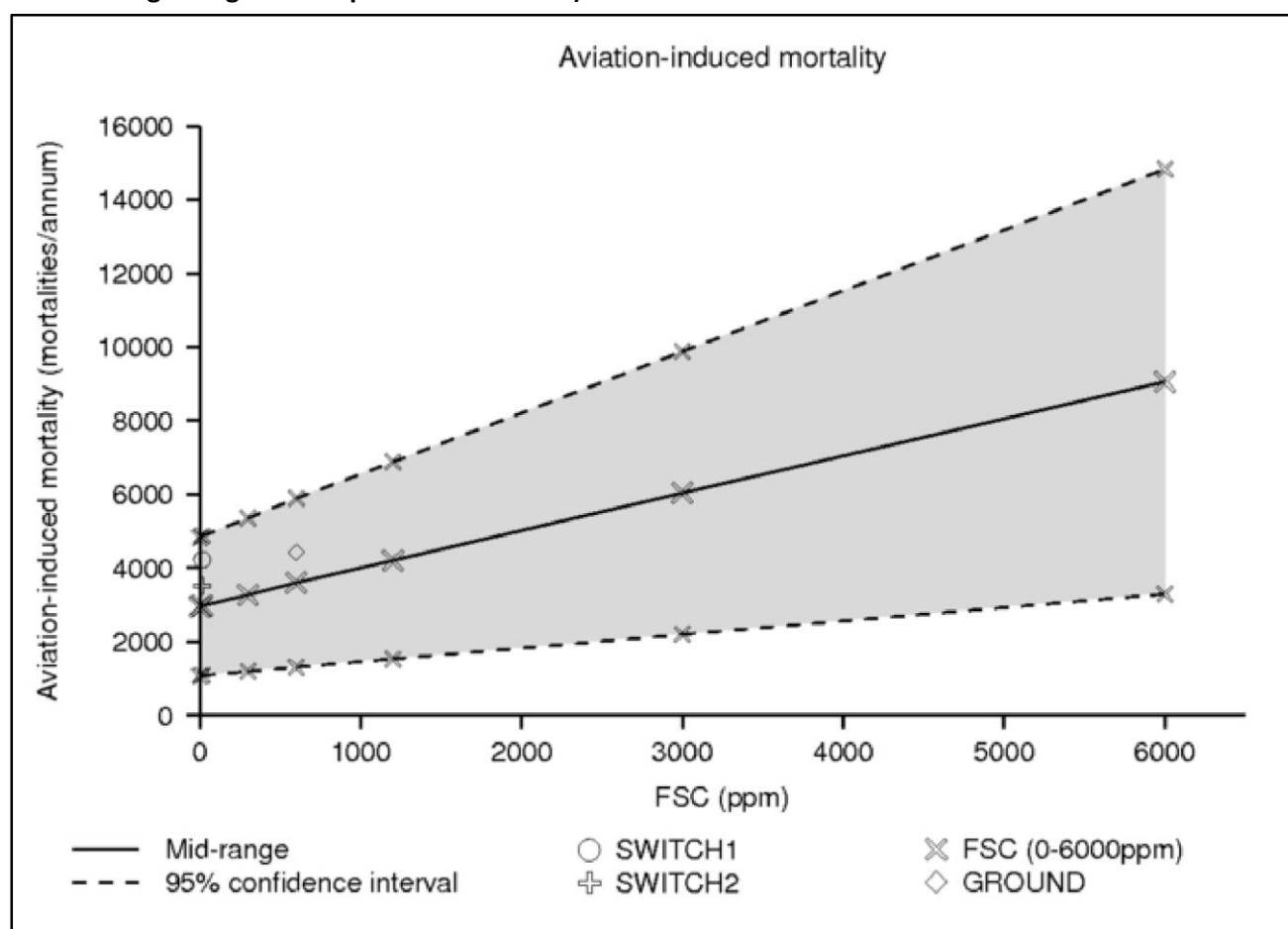
achieved through reducing FSC alone, with further reductions in aviation-induced PM_{2.5} sulfates requiring additional controls on aviation NO_x emissions.

3.2 Premature mortality

Fig. 6 shows estimated annual premature mortalities (from cardiopulmonary disease and lung cancer) due to aviation-induced changes in PM_{2.5} as a function of FSC. We estimate that aviation emissions with standard FSC (FSC = 600 ppm) cause 3,600 [95% CI: 1,310–5,890] premature mortalities each year, with 3210 [95% CI: 1160–5250] mortalities a⁻¹ due to increases in cases of cardiopulmonary disease and 390 [95% CI: 150–640] mortalities a⁻¹ due to increases in cases of lung cancer. Low-, mid- and high-range cause-specific coefficients (β) are used to account for uncertainty in the health impacts caused by exposure to PM_{2.5} (Section 2.5) (Ostro, 2004). Our estimated global mortality due to aviation emissions is greatest in the Northern Hemisphere, which accounts for 98.7% of global mortalities. Europe and North America account for 42.3% and 8.4% of mortality due to aviation emissions respectively.

Our estimate of the premature mortality due to aviation lies within the range of previous estimates (310–13,920 mortalities a⁻¹) (Barrett et al., 2010; Barrett et al., 2012; Jacobson et al., 2013; Morita et al., 2014; Yim et al., 2004). Barrett et al. (2012) estimated ~10,000 mortalities a⁻¹ due to aviation, almost a factor 3 higher than our central estimate. The greater aviation-induced mortality simulated by Barrett et al. (2012), can be attributed to greater aviation-induced surface PM_{2.5} concentrations simulated in their study, particularly over highly populated areas. Their study simulated maximum aviation-induced PM_{2.5} concentrations over Europe, eastern China and eastern North America greater than those in our simulations by factors of 5 for Europe and eastern China and 2.5 over eastern North America. Our aviation-induced sulfate concentrations compare well with Barrett et al. (2012), indicating that the resulting differences in aviation-induced surface PM_{2.5} concentrations are a result of other aerosol components. Additionally, differences in mortality arise due to the use of different cause-specific coefficients (β) within the same CRF, as well as different population datasets. Morita et al. (2014) estimate that aviation is responsible for 405 [95% CI: 182–648] mortalities a⁻¹. This lower estimate is primarily due to the mortality functions used, with Morita et al. (2014) using the integrated exposure response (IER) function as described by Burnett et al. (2014). The IER function considers a PM_{2.5} concentration below which there is no perceived risk, reducing estimated impacts of aviation in regions of low PM_{2.5} concentrations.

535 **Fig. 6: Estimated global aviation-induced mortality as a function of FSC, and changes in vertical aviation-**
536 **emissions distributions for year 2000 (Shaded region denotes the 95% confidence through application of**
537 **low- and high-range cause-specific coefficients).**



538 We estimate that aviation emissions with ULSJ fuel result in 2,970 [95% CI: 1,080–4,870] premature mortalities
539 globally per annum. Therefore, changing from standard FSC to ULSJ would result in 620 [95% CI: 230–1,020]
540 fewer premature mortalities globally per annum; a reduction in aviation-induced mortalities of 17.4%.
541 Regionally we find the implementation of an ULSJ fuel reduces annual mortality by 180 over Europe and by
542 110 over North America.

543
544 Barrett et al. (2012) estimated that swapping to ULSJ fuel could result in ~2,300 [95% CI: 890–4,200] fewer
545 premature mortalities globally per annum; a reduction of 23%. In their work (using GEOS-Chem), the use of
546 ULSJ reduces global mean PM_{2.5} concentrations (sulfates, nitrates and ammonium) by 0.89 ng m⁻³, less than
547 the 1.61 ng m⁻³ reduction in PM_{2.5} simulated here). Despite the greater reductions in global mean surface layer
548 PM_{2.5} concentrations simulated here, Barrett et al. (2012) simulate greater reductions in PM_{2.5} over populated
549 regions, resulting in greater reductions of aviation-induced mortality under the ULSJ scenario. Additionally,
550 the GRUMPv1 population dataset that Barrett et al. (2012) use resolves population data on a finer scale
551 compared to the resolution of GPWv3 population dataset used here (Center for International Earth Science
552 Information Network, 2012); differences which could contribute to differences in estimates of mortality.

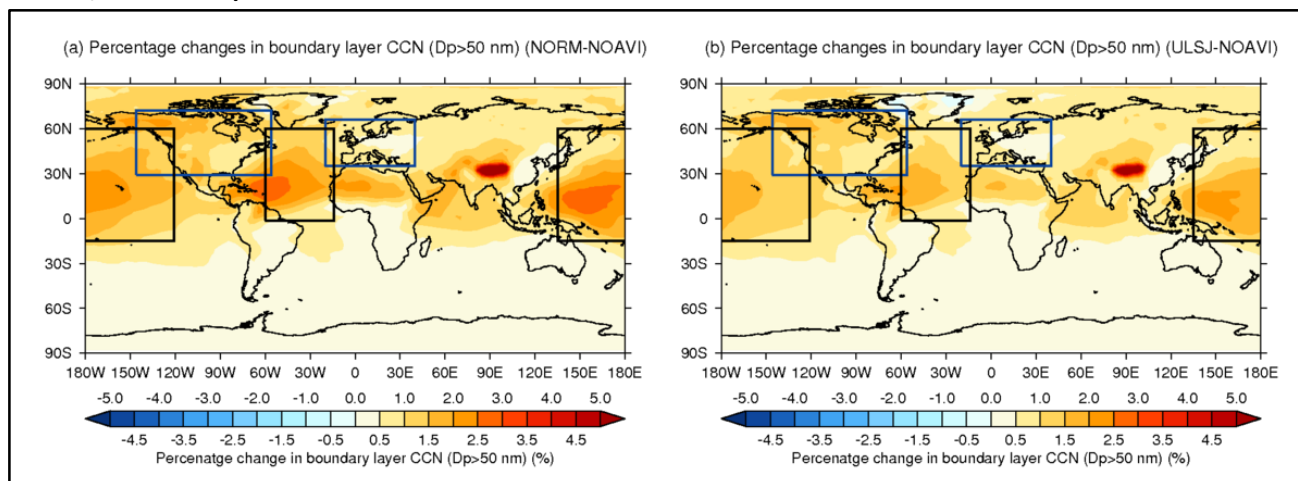
553
554 We also estimate how aviation-induced mortality would change if FSC was increased. We find that increasing
555 FSC to 3000 ppm (HIGH) would increase annual aviation-induced mortalities to 6,030, an increase of 67.8% in
556 relation to standard aviation (NORM; FSC = 600 ppm).

558 3.3 Sensitivity of cloud condensation nuclei to aviation FSC

559 Aviation emissions with standard FSC (NORM; FSC = 600 ppm) increase global annual mean cloud condensation
560 nuclei (CCN), here taken as the number of soluble particles with a dry diameter greater than 50 nm, at low-

cloud level (879hPa; 0.96km) by 0.9% (2.3 cm^{-3}) (Fig. 7(a)). Increases in CCN concentrations are greater in the Northern Hemisphere [$+3.9 \text{ cm}^{-3}$; $+1.4\%$] compared to the Southern Hemisphere [$+0.7 \text{ cm}^{-3}$; $+0.5\%$]. Maximum increases in low-level CCN are simulated over the Pacific, central Atlantic and Arctic Oceans.

Fig. 7: Impact of aviation emissions on low-cloud level (879 hPa) CCN ($D_p > 50 \text{ nm}$) concentrations: (a) standard FSC (NORM–NOAVI) and (b) FSC = 15 ppm (ULSJ–NOAVI). Blue boxes define North American and European regions, and black boxes define Atlantic (60°W – 14°W , 1.4°S – 60°N) and Pacific regions (135°E – 121°W , 15°S – 60°N) referred to in the text.



The use of ULSJ (FSC = 15 ppm) reduces global mean low-level CCN concentrations by 0.4 cm^{-3} , $[-18.2\%]$ relative to the NORM case (Fig. 7). Northern Hemisphere CCN concentrations are reduced by 0.8 cm^{-3} $[-19.4\%]$, while Southern Hemisphere concentrations are reduced by 0.1 cm^{-3} $[-11.5\%]$ (Fig. 7).

Fig. 8: Global and regional variations in low-cloud level (879 hPa) CCN ($D_p > 50 \text{ nm}$): (a) changes in mean concentrations and (b) percentage changes. See Fig. 5 for definitions of regions.

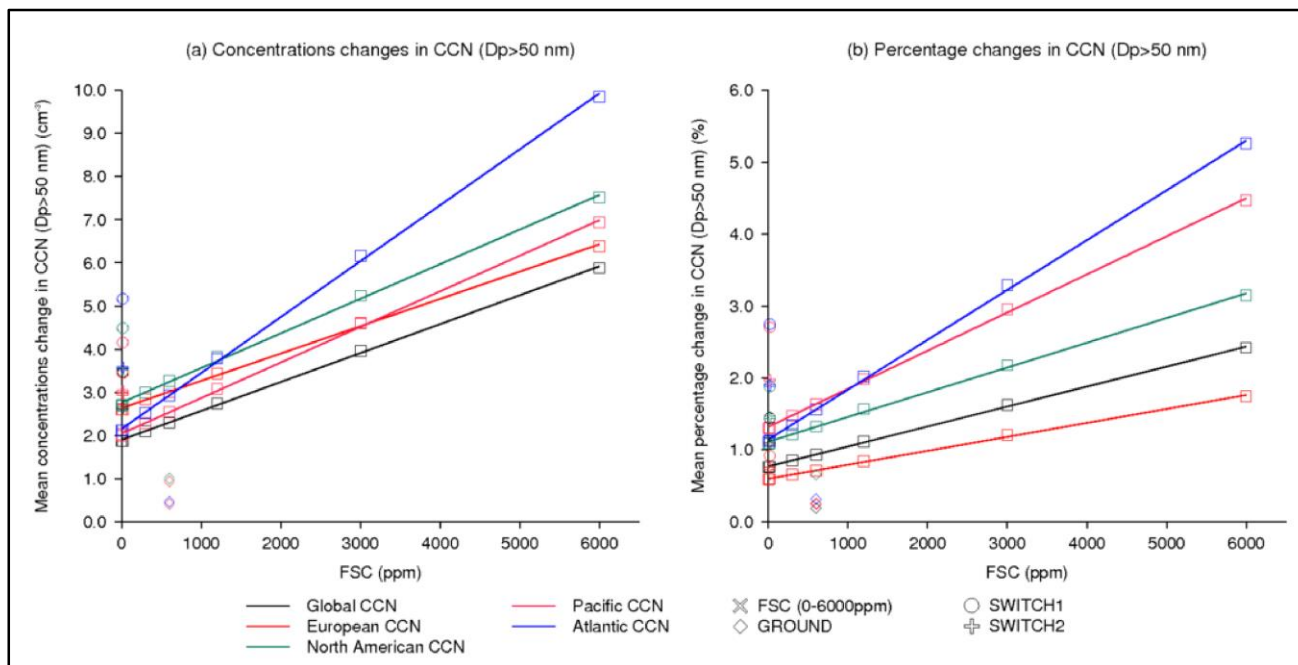


Fig. 8 shows the sensitivity of low level CCN concentrations to FSC. As with $\text{PM}_{2.5}$, we find simulated changes in CCN are near linear with respect to FSC ($R^2 > 0.99$ and $p\text{-value} < 0.001$ globally and for all individual regions).

ULSJ fuel reduces global mean CCN by -0.42 cm^{-3} with largest reductions over the Atlantic Ocean $[-0.81 \text{ cm}^{-3}]$, North America $[-0.55 \text{ cm}^{-3}]$, and the Pacific Ocean $[-0.51 \text{ cm}^{-3}]$, i.e. in relation to standard aviation (ULSJ–NORM). The complete desulfurisation of aviation fuel results in reductions in CCN in relation to standard aviation (DESUL–NORM), which follow the same regional trends (Fig. 8(a)).

582

583 **3.4 Sensitivity of aerosol and ozone radiative effect to FSC**

584

585 Fig. 9 shows the calculated global mean net RE due to non-CO₂ aviation emissions. For standard FSC (FSC = 600

586 ppm) emissions the global mean combined RE is -13.3 mW m^{-2} . This combined radiative effect (RE_{comb}) results

587 from a balance between a positive aDRE of $+1.4 \text{ mW m}^{-2}$ and O3DRE $+8.9 \text{ mW m}^{-2}$, and a negative aCAE of $-$

588 23.6 mW m^{-2} (Fig. 9).

589

590 Our estimated aviation aerosol DRE [$+1.4 \text{ mW m}^{-2}$] lies in the middle of the range given by previous work. The

591 aviation aerosol DRE has been previously assessed as highly uncertain, ranging between -28 to $+20 \text{ mW m}^{-2}$

592 (Righi et al., 2013). Our estimated aviation-induced aCAE [-23.6 mW m^{-2}] lies within the range of uncertainty

593 from previous literature: Righi et al. (2013) estimated $-15.4 \pm 10.6 \text{ mW m}^{-2}$ and Gettelman and Chen (2013)

594 estimated $-21 \pm 11 \text{ mW m}^{-2}$.

595

596 Our O3DRE estimate ($+8.9 \text{ mW m}^{-2}$), normalised by global aviation NO_x emission to $+10.5 \text{ mW m}^{-2} \text{ Tg(N)}^{-1}$, is at

597 the lower end of current estimates [$7.4\text{--}37.0 \text{ mW m}^{-2} \text{ Tg(N)}^{-1}$] (Sausen et al., 2005; Köhler et al., 2008; Hoor et

598 al., 2009; Lee et al., 2009; Holmes et al., 2011; Myhre et al., 2011; Unger, 2011; Frömming et al., 2012; Skowron

599 et al., 2013; Unger et al., 2013; Khodayari et al., 2014). This can be attributed to the lower net O₃ chemical

600 production efficiency (OPE) within our model (1.33). Unger (2011) estimated an O3DRE of $7.4 \text{ mW m}^{-2} \text{ Tg(N)}^{-1}$

601 with a model OPE of ~ 1 , while the ensemble of models considered by Myhre et al. (2011) have an OPE range

602 of $1.5\text{--}2.4$, resulting in an O3DRE range of $16.2\text{--}25.4 \text{ mW m}^{-2} \text{ Tg(N)}^{-1}$.

603

604 We calculate that an aviation fleet utilising ULSJ fuel would result in a in a global annual mean RE_{comb} of -6.3

605 mW m^{-2} [aDRE = $+1.8 \text{ mW m}^{-2}$; aCAE = -16.8 mW m^{-2} ; and O3DRE = $+8.7 \text{ mW m}^{-2}$]. Thus, swapping from

606 standard aviation fuel to ULSJ fuel reduces the net cooling effect from aviation-induced aerosol and O₃ by 7.0

607 mW m^{-2} , in comparison to the reduction of 3.3 mW m^{-2} estimated by Barrett et al. (2012). In our model, this

608 change is primarily due a reduction in cooling from the aCAE of $+6.7 \text{ mW m}^{-2}$ combined with smaller

609 contributions from an increased aDRE of $+0.4 \text{ mW m}^{-2}$, and reduction in warming from the O3DRE of -0.12

610 mW m^{-2} (Fig. 9).

611

612 When we assume fully desulfurised aviation jet fuel (DESUL; FSC = 0 ppm), the RE_{comb} induced by aviation-

613 induced aerosol and O₃ is very similar to that for ULSJ fuel and is estimated as -6.1 mW m^{-2} [aDRE = $+1.8 \text{ mW}$

614 m^{-2} ; aCAE = -16.6 mW m^{-2} ; and O3DRE = $+8.7 \text{ mW m}^{-2}$].

615

616

617

618

619

620

621

622

623

624

625

626

627

628

629

630

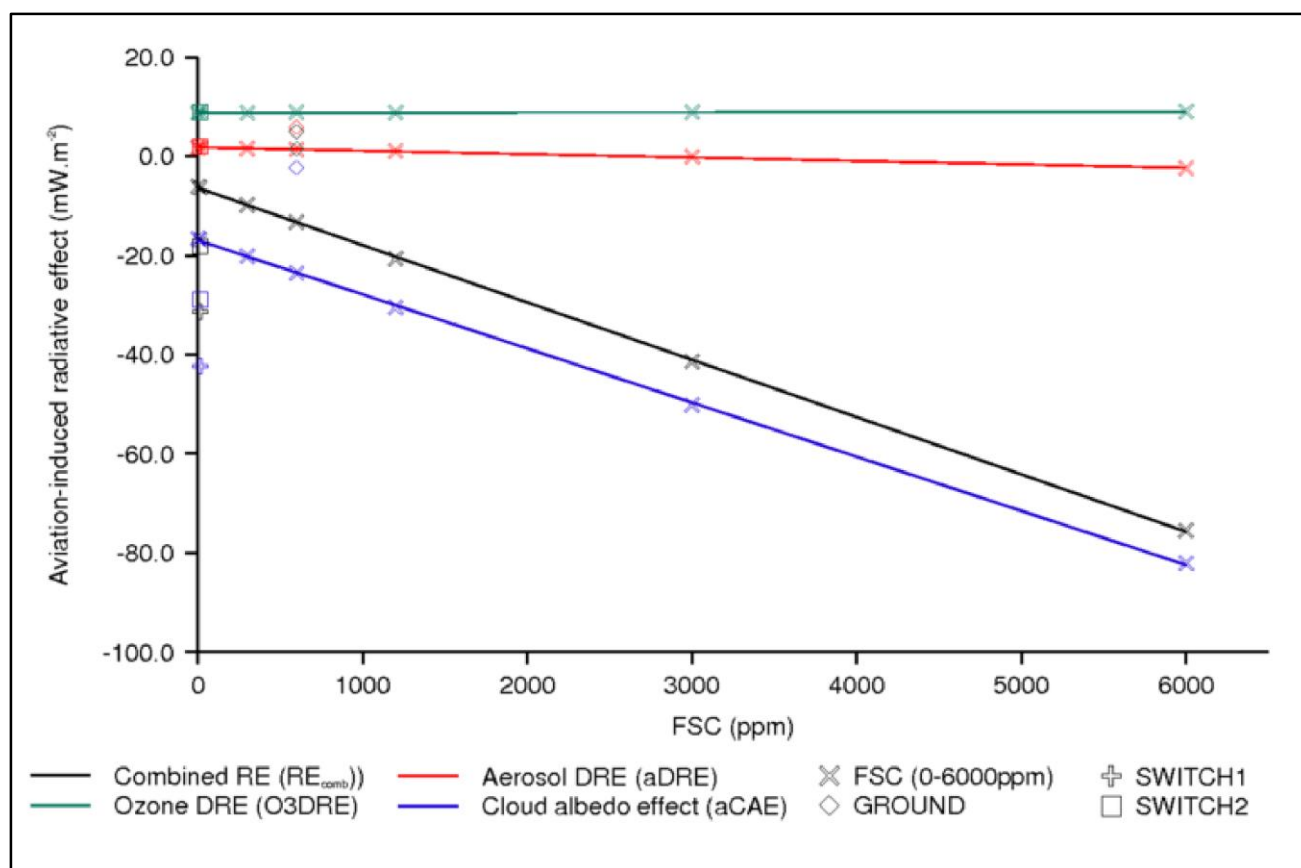
631

632

633

634

635 **Fig. 9: Aviation-induced radiative effects due to variations in fuel sulfur content (FSC), the ground release of**
 636 **aviation emissions (GROUND), and variations in the vertical distribution of aviation SO₂ emissions (SWITCH1**
 637 **and SWITCH2 simulations).**

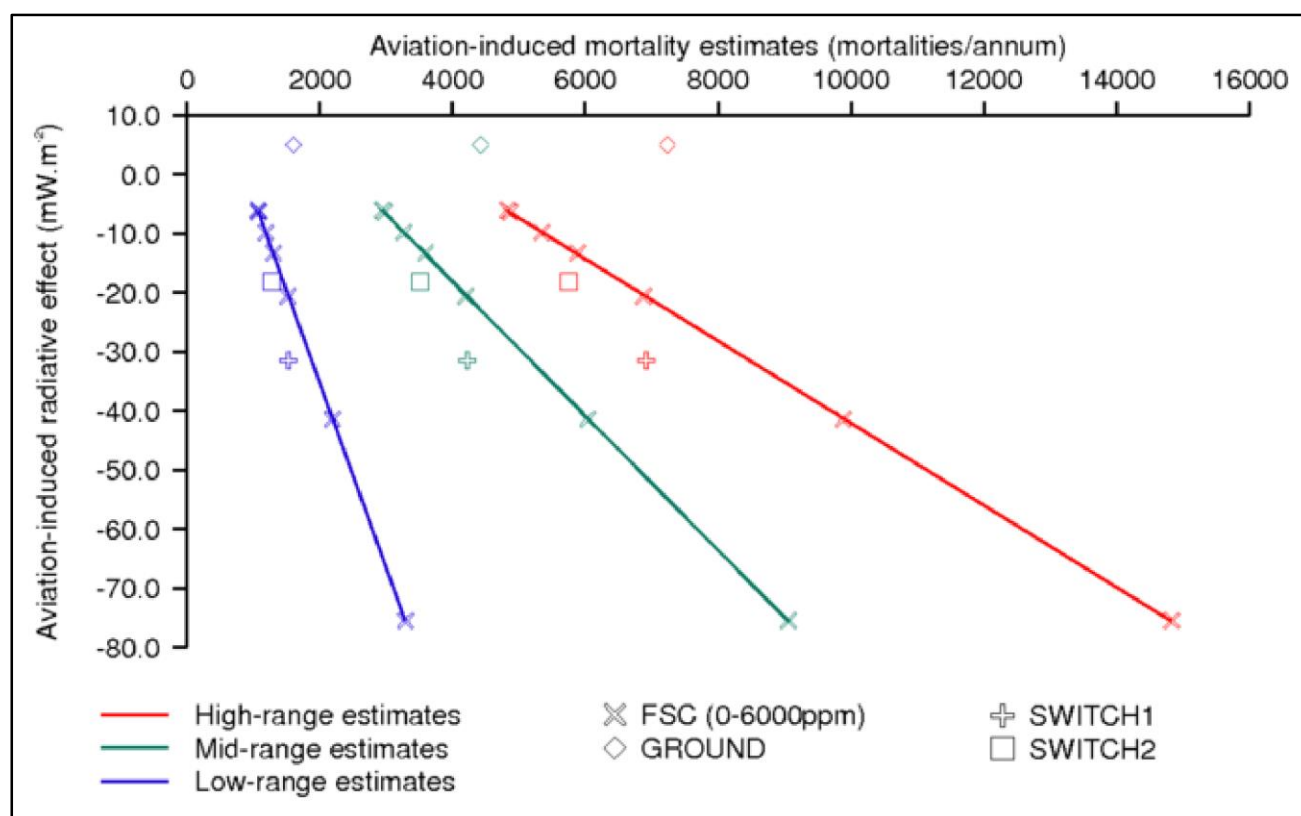


638 Increases in FSC result in reductions in the aerosol DRE (aDRE), changing from a positive aerosol DRE for low
 639 FSC scenarios, to a negative aerosol DRE for high FSC (FSC > 1200 ppm). As FSC is increased, we find the aCAE
 640 exhibits a larger cooling effect, i.e. becoming more negative with increases in FSC, increasing by a factor ~5 as
 641 FSC is increased from 0 to 6000 ppm. The RE_{comb} is dominated by these changes to the aCAE. As a result
 642 increases in FSC from 0–6000 ppm, result in a greater negative (cooling) aviation-induced RE_{comb}; increasing in
 643 magnitude by a factor of ~5 (–16.6 mW m⁻² for FSC = 0 ppm to –82.1 mW m⁻² for FSC = 6000 ppm) (Fig. 9).
 644 Therefore, we find that increases in FSC provide a cooling effect due to the dominating effect from aviation-
 645 induced aCAE.

647 3.5 Relationship between aviation-induced radiative effects and mortality due to aviation 648 non-CO₂ emissions

649 Fig. 10 shows the net RE and premature mortality for different aviation emission scenarios. Increases in FSC
 650 lead to approximately linear increases in both estimated mortality and the negative net RE. We quantify the
 651 impact of FSC on mortality and REs in terms of d(mortalities)/d(FSC) [mortalities ppm⁻¹] and d(RE)/d(FSC) [mW
 652 m⁻² ppm⁻¹]. We calculate the sensitivity of global premature mortality to be 1.0 mortalities ppm⁻¹ [95% CI = 0.4
 653 to 1.6 mortalities ppm⁻¹, where the range is due to uncertainty in β]. The global mean RE_{comb} has a sensitivity
 654 of –1.2x10⁻² mW m⁻² ppm⁻¹, dominated by large changes to the aCAE [–1.1x10⁻² mW m⁻² ppm⁻¹], and much
 655 smaller changes in the aDRE [–6.9x10⁻⁴ mW m⁻² ppm⁻¹] and O₃ RE [+4.4x10⁻⁵ mW m⁻² ppm⁻¹].

663 **Fig. 10: Relationship between net radiative effect [sum of ozone direct (O3DRE), aerosol direct radiative**
664 **(aDRE) and aerosol cloud albedo (aCAE) effects] and annual mortality rates: for low- mid- and high-range**
665 **mortality sensitivities.**



666 The different slopes in the relationship between estimated RE and mortality (Fig. 10) are driven by the range
667 of coefficients used in the CRF. This highlights the considerable uncertainty in the health impacts caused by
668 exposure to PM_{2.5}. We note that uncertainty in the RE due to aerosol and ozone exists, but is not included in
669 Fig. 9.

670
671 To assess how the vertical distributions of aviation SO₂ emissions influence human health and climate effects,
672 we performed three additional simulations where we altered the vertical distribution of aviation SO₂ emissions
673 (GROUND, SWITCH1 and SWITCH2 simulations). In these simulations the relationships between mortality and
674 net RE deviate from the linear relationship seen when varying FSC between 0–6000 ppm (Fig. 10).

675
676 In relation to the standard aviation emissions simulation (FSC = 600 ppm; NORM), when we release all aviation
677 emissions at the surface (GROUND; FSC = 600 ppm) aviation-induced surface PM_{2.5} concentrations increase by
678 +13.5 ng m⁻³ [+65.7%] over Europe and by +1.7 ng m⁻³ [+27.1%] over North America, but decrease by -1.4 ng
679 m⁻³ [-36.7%] globally (Fig. 4). Greater surface layer PM_{2.5} perturbations (GROUND–NORM) over populated
680 regions increase aviation-induced annual mortality by +22.9% [+830 mortalities a⁻¹] (Fig. 6).

681
682 Releasing aviation emissions at the surface (GROUND case) increases global mean cloud level CCN by only 0.4
683 cm⁻³ relative to NOAVI; providing a reduction in CCN of 82.1% [-1.89 cm⁻³] relative to the NORM case (i.e.
684 GROUND–NORM). That is, injecting aviation emissions into the free troposphere in the standard scenario is
685 over 5 times more efficient at increasing CCN concentrations compared to when the same emissions are
686 released at the surface [GROUND CCN = 0.4 cm⁻³; NORM CCN = 2.3 cm⁻³]; both in relation to the NOAVI
687 scenario. Similar behaviour has been demonstrated previously for volcanic SO₂ emissions by Schmidt et al.
688 (2012), where volcanic SO₂ emissions injected into the free troposphere (FT) were more than twice as effective
689 at producing new CCN compared to boundary layer emissions of DMS. Injection of aviation SO₂ emissions at
690 the surface will increase both deposition rates and aqueous phase oxidation of SO₂; the latter resulting in the
691 growth of existing CCN, but not the formation of new CCN. In contrast, when SO₂ is emitted into the FT the
692 dominant oxidation mechanism is to H₂SO₄, leading to the formation of new CCN through particle formation

and the condensational growth of particles to larger sizes. Subsequent entrainment of these new particles into the lower atmosphere results in enhanced CCN concentrations in low level clouds. Reduced CCN formation when aviation emissions are injected at the surface has implications for the aCAE. When aviation emissions are released at the surface we calculate an aCAE of -2.3 mW m^{-2} ; a factor of 10 smaller than the standard aviation scenario. This demonstrates that low-level CCN concentrations and the aCAE are particularly sensitive to aviation emissions, because of the efficient formation of CCN when SO_2 emissions are injected into the FT. Injecting aviation emissions at the surface also results in an increase in the aDRE of $+5.9 \text{ mW m}^{-2}$, resulting in a RE_{comb} of $+5.0 \text{ mW m}^{-2}$ (Fig. 9).

Surface O_3 concentrations are also less sensitive to aviation when emissions are located at the surface. Global mean aviation-induced surface O_3 concentrations are reduced from 0.15 ppbv (NORM) to 0.03 ppbv when all emissions are in the surface layer. Releasing aviation emissions at the surface also reduces the global O_3 burden by 3.1 Tg. These perturbations in O_3 concentrations result in a reduction in the O_3 radiative effect from $+8.9 \text{ mW m}^{-2}$ (NORM; FSC = 600 ppm) to $+1.5 \text{ mW m}^{-2}$ (GROUND; FSC = 600 ppm) (Fig. 9). This is a reflection of increases in the OPE of NO_x with increases in altitude due to lower background NO_x and NMHC (non-methane hydrocarbon) concentrations (Köhler et al., 2008; Stevenson and Derwent, 2009; Snijders and Melkers, 2011; Skowron et al., 2013).

We investigated altering FSC between the take-off / landing and the cruise phases of flight using two scenarios (SWITCH1 and SWITCH2) (Table 2). Our SWITCH1 scenario increases global mean aviation-induced surface layer $\text{PM}_{2.5}$ concentrations by $+2.1 \text{ ng m}^{-3}$ [52.2%], European mean concentrations by $+0.9 \text{ ng m}^{-3}$ [+4.5%], and North American concentrations by $+2.7 \text{ ng m}^{-3}$ [+42.2%] relative to NORM (Fig. 4). These changes increase aviation-induced mortality by $+17.4\%$ [+630 mortalities a^{-1}] (Fig. 6). This scenario results in greater global mean increases in CCN (relative to NORM) of $+1.2 \text{ cm}^{-3}$ [+51.2%], a larger cooling aCAE [-42.4 mW m^{-2}], larger warming aDRE [2.07 mW m^{-2}], resulting in additional -18.1 mW m^{-2} [136%] of aviation-induced cooling [SWITCH1 RE_{comb} of -31.4 mW m^{-2}].

The SWITCH2 scenario was designed to have the same global total sulfur emission as the normal aviation simulation. SWITCH2 increased global mean surface aviation-induced $\text{PM}_{2.5}$ concentrations by $+0.3 \text{ ng m}^{-3}$ [+6.6%], but reduces mean surface $\text{PM}_{2.5}$ concentrations over Europe [-1.8 ng m^{-3} ; -8.7%] and North America [-0.8 ng m^{-3} ; -12.8%] compared to NORM. Under this scenario global aviation-induced mortality is decreased by 2.4% [-90 mortalities a^{-1}] compared to the standard aviation simulation (Fig. 6). The SWITCH2 scenario results in a RE_{comb} of -18.2 mW m^{-2} , providing an additional -4.9 mW m^{-2} [36.6%] cooling in relation to standard aviation emissions (NORM; FSC = 600 ppm).

4 Discussion and Conclusions

We have used a coupled chemistry-aerosol microphysics model to estimate the impact of aviation emissions on aerosol and O_3 concentrations, premature mortality and radiative effect on climate.

We calculated the top-of-atmosphere (TOA) tropospheric O_3 radiative effect (O3DRE), aerosol direct RE (aDRE) and aerosol cloud albedo effect (aCAE). We find that these non- CO_2 REs result in a net cooling effect on climate as has been found previously (Sausen et al., 2005; Lee et al., 2009; Gettelman and Chen, 2013; Righi et al., 2013; Unger et al., 2013). For year 2000 aviation emissions with a standard fuel sulfur content (FSC = 600 ppm), we calculate a global annual mean net TOA RE of -13.3 mW m^{-2} , due to a combination of O3DRE [$+8.9 \text{ mW m}^{-2}$], aDRE [$+1.4 \text{ mW m}^{-2}$] and aCAE [-23.6 mW m^{-2}].

Our O3DRE [$+8.9 \text{ mW m}^{-2}$] when normalised to represent the impact of the emissions of $1\text{Tg}(\text{N})$ [$+10.45 \text{ mW m}^{-2} \text{Tg}(\text{N})^{-1}$] is at the lower end of range provided by previous studies [$7.39\text{--}36.95 \text{ mW m}^{-2} \text{Tg}(\text{N})^{-1}$] (Sausen et al., 2005; Hoor et al., 2009; Lee et al., 2009; Holmes et al., 2011; Myhre et al., 2011; Unger, 2011; Frömming et al., 2012; Unger et al., 2013; Khodayari et al., 2014). This can be attributed to our model's lower OPE of 1.33, in comparison to the range of 1–2.4 from other models (Myhre et al., 2011; Unger, 2011).

Our estimate of aviation-induced aCAE [-23.6 mW m^{-2}] lies just outside the range provided by Gettelman and Chen (2013) and Righi et al. (2013) [-15.4 to -21 mW m^{-2}]. Our estimated aDRE [$+1.4 \text{ mW m}^{-2}$] lies within the middle of the range given by previous work (Sausen et al., 2005; Fuglestad et al., 2008; Lee et al., 2009; Balkanski et al., 2010; Unger, 2011; Gettelman and Chen, 2013; Righi et al., 2013; Unger et al., 2013).

We estimate that standard aviation (NORM; FSC = 600 ppm) is responsible for approximately 3,600 premature mortalities annually due to increased surface layer $\text{PM}_{2.5}$, in line with previous work (Barrett et al., 2012). We find that aviation-induced mortalities are highest over Europe, eastern North America and eastern China; reflecting larger regional perturbations in surface layer $\text{PM}_{2.5}$ concentrations. Comparing these estimates with total global premature mortalities from ambient air pollution from all anthropogenic sources (Lim et al., 2012), aviation is responsible for 0.1% [0.04–0.18%] of annual premature mortalities.

We investigated the impact of varying aviation FSC over the range 0–6000 ppm. Increases in FSC lead to increases in surface $\text{PM}_{2.5}$ concentrations and subsequent increases in aviation-induced mortality. Increases in FSC also lead to a more negative RE_{comb} due to an enhanced aCAEs. We estimate that the use of ultra-low sulfur jet (ULSJ) fuel, with a FSC of 15 ppm, could prevent 620 [230–1,020] mortalities annually compared to standard aviation emissions. Swapping to ULSJ fuel increases the global mean net RE by $+7.0 \text{ mW m}^{-2}$ compared to standard aviation emissions, largely due to a reduced aCAE. We calculate a larger warming effect from switching to ULSJ fuel than that assessed by Barrett et al. (2012), who did not evaluate changes in aCAE.

Absolute reductions in FSC result in limited reductions in aviation-induced surface layer $\text{PM}_{2.5}$. We estimate that aviation- NO_x emissions are responsible for 36.2% of aviation-induced sulfate perturbations. Thus further reductions in aviation-induced $\text{PM}_{2.5}$ can potentially be achieved if NO_x emission reductions are implemented in tandem with reductions to fuel sulfur content.

In line with previous work (Köhler et al., 2008; Stevenson and Derwent, 2009; Snijders and Melkers, 2011; Frömming et al., 2012; Skowron et al., 2013), decreasing the altitude at which O_3 forming species are emitted results in a reduction in aviation-induced O_3 , and resulting O3DRE. This is due to the relationship between altitude and OPE, and the inverse relationship between altitude and background pollutant concentrations. We also explored the sensitivity of emission injection altitude on aerosol, mortality and aerosol RE. Injecting aviation emissions at the surface results in a reduction in global mean concentrations of $\text{PM}_{2.5}$ (relative to NORM), but with higher regional concentrations over central Europe and eastern America; resulting in higher annual mortalities due to aviation. We find that aviation emissions are a factor of 5 less efficient at creating CCN when released at the surface, resulting in an aCAE of -2.3 mW m^{-2} , a reduction of 90.1% in relation to the standard aviation scenario. When aviation SO_2 emissions are injected into the free-troposphere, the dominant oxidation pathway is to H_2SO_4 followed by particle formation and condensational growth of new particles to larger sizes. Subsequent entrainment of these new particles into the lower atmosphere leads to increased CCN concentrations and impacts on cloud albedo. Aviation SO_2 emissions are therefore particularly efficient at forming CCN with resulting impacts on cloud albedo.

We explored the impact of applying altitude dependent variations in aviation FSC. We tested a scenario with high FSC in the free troposphere and low FSC near the surface, resulting in the same global aviation sulfur emission as the standard aviation scenario. In this scenario, aviation-induced premature mortalities were reduced by 2.4% [-90 mortalities a^{-1}] and the magnitude of the negative RE_{comb} was increased by 36.6%, providing an additional cooling impact of climate of -4.88 mW m^{-2} .

Our simulations suggest that the climate and air quality impacts of aviation are sensitive to FSC and the altitude of emissions. We explored a range of scenarios to maximise climate cooling and reduce air quality impacts. Use of ULSJ fuel (FSC = 15 ppm) at low altitude combined with high FSC in the free troposphere results in increased climate cooling whilst reducing aviation mortality. More complicated emission patterns, for example, use of high FSC only whilst over oceans might further enhance this effect. However, we note that the greatest reduction in aviation-induced mortality is simulated for complete desulfurisation of aviation fuel. Given the uncertainty in both the climate and air quality impacts of aerosol and ozone, additional simulations from a range of atmospheric models are required to explore the robustness of our calculations. Finally, we

800 note that our calculations are limited to calculation of aviation-induced RE. Future work needs to assess the
801 complex climate impacts of altering aviation FSC. Future work needs to estimate the health impacts of aviation
802 using newly available concentration response functions (Burnett et al., 2014).
803

804 **Author information**

805 *Phone: 0113 343 8167. E-mail: pm08zzk@leeds.ac.uk
806

807 **Acknowledgements**

808 The authors acknowledge the Engineering & Physical Sciences Research Council (EPSRC) for funding of Z Z
809 Kapadia through the EPSRC Doctoral Training Centre in Low Carbon Technologies (EPSRC Grant
810 EP/G036608/1).
811

812 The authors are also grateful to Jean-Francois Lamarque and the ‘Historical emissions group’ and IIASA for
813 their publically available recommended historical CMIP5 aviation emissions data.
814

815 **References**

- 816 Airbus: A318/A319/A320/A321 FCTM (Flight Crew Training Manual), FCA A318/A319/A320/A321 FLEET,
817 2008.
- 818 Anderson, B. E., Chen, G., and Blake, D. R.: Hydrocarbon emissions from a modern commercial airliner,
819 Atmospheric Environment, 40, 3601-3612, <http://dx.doi.org/10.1016/j.atmosenv.2005.09.072>, 2006.
- 820 Andres, R. J., and Kasgnoc, A. D.: A time-averaged inventory of subaerial volcanic sulfur emissions, Journal of
821 Geophysical Research: Atmospheres, 103, 25251-25261, 10.1029/98JD02091, 1998.
- 822 Arnold, S. R., Chipperfield, M. P., and Blitz, M. A.: A three-dimensional model study of the effect of new
823 temperature-dependent quantum yields for acetone photolysis, Journal of Geophysical Research:
824 Atmospheres, 110, D22305, 10.1029/2005JD005998, 2005.
- 825 ASTM International: D1655-11b: Standard Specification for Aviation Turbine Fuels, ASTM International, West
826 Conshohocken, PA, United States, 2012.
- 827 Balkanski, Y., Myhre, G., Gauss, M., Rädel, G., Highwood, E. J., and Shine, K. P.: Direct radiative effect of
828 aerosols emitted by transport: from road, shipping and aviation, Atmos. Chem. Phys., 10, 4477-4489,
829 10.5194/acp-10-4477-2010, 2010.
- 830 Barahona, D., West, R. E. L., Stier, P., Romakkaniemi, S., Kokkola, H., and Nenes, A.: Comprehensively
831 accounting for the effect of giant CCN in cloud activation parameterizations, Atmos. Chem. Phys., 10, 2467-
832 2473, 10.5194/acp-10-2467-2010, 2010.
- 833 Barrett, S. R. H., Britter, R. E., and Waitz, I. A.: Global Mortality Attributable to Aircraft Cruise Emissions,
834 Environmental Science & Technology, 44, 7736-7742, 10.1021/es101325r, 2010.
- 835 Barrett, S. R. H., Yim, S. H. L., Gilmore, C. K., Murray, L. T., Kuhn, S. R., Tai, A. P. K., Yantosca, R. M., Byun, D.
836 W., Ngan, F., Li, X., Levy, J. I., Ashok, A., Koo, J., Wong, H. M., Dessens, O., Balasubramanian, S., Fleming, G.
837 G., Pearlson, M. N., Wollersheim, C., Malina, R., Arunachalam, S., Binkowski, F. S., Leibensperger, E. M.,
838 Jacob, D. J., Hileman, J. I., and Waitz, I. A.: Public Health, Climate, and Economic Impacts of Desulfurizing Jet
839 Fuel, Environmental Science & Technology, 46, 4275-4282, 10.1021/es203325a, 2012.
- 840 Benduhn, F., Mann, G. W., Pringle, K. J., Topping, D. O., McFiggans, G., and Carslaw, K. S.: Size-resolved
841 simulations of the aerosol inorganic composition with the new hybrid dissolution solver HyDiS-1.0 –
842 Description, evaluation and first global modelling results, Geosci. Model Dev. Discuss., 2016, 1-54,
843 10.5194/gmd-2015-264, 2016.
- 844 Bond, T. C., Streets, D. G., Yarber, K. F., Nelson, S. M., Woo, J.-H., and Klimont, Z.: A technology-based global
845 inventory of black and organic carbon emissions from combustion, Journal of Geophysical Research:
846 Atmospheres, 109, D14203, 10.1029/2003JD003697, 2004.
- 847 Bouwman, A. F., Lee, D. S., Asman, W. A. H., Dentener, F. J., Van Der Hoek, K. W., and Olivier, J. G. J.: A global
848 high-resolution emission inventory for ammonia, Global Biogeochemical Cycles, 11, 561-587,
849 10.1029/97GB02266, 1997.

850 Brasseur, G. P., Gupta, M., Anderson, B. E., Balasubramanian, S., Barrett, S., Duda, D., Fleming, G., Forster, P.
851 M., Fuglestad, J., Gettelman, A., Halthore, R. N., Jacob, S. D., Jacobson, M. Z., Khodayari, A., Liou, K.-N.,
852 Lund, M. T., Miake-Lye, R. C., Minnis, P., Olsen, S., Penner, J. E., Prinn, R., Schumann, U., Selkirk, H. B.,
853 Sokolov, A., Unger, N., Wolfe, P., Wong, H.-W., Wuebbles, D. W., Yi, B., Yang, P., and Zhou, C.: Impact of
854 Aviation on Climate: FAA's Aviation Climate Change Research Initiative (ACCRI) Phase II, Bulletin of the
855 American Meteorological Society, 10.1175/BAMS-D-13-00089.1, 2015.

856 Breider, T. J., Chipperfield, M. P., Richards, N. A. D., Carslaw, K. S., Mann, G. W., and Spracklen, D. V.: Impact
857 of BrO on dimethylsulfide in the remote marine boundary layer, Geophysical Research Letters, 37, L02807,
858 10.1029/2009GL040868, 2010.

859 Burkhardt, U., and Karcher, B.: Global radiative forcing from contrail cirrus, Nature Clim. Change, 1, 54-58,
860 2011.

861 Burnett, R. T., Pope, C. A., Ezzati, M., Olives, C., Lim, S. S., Mehta, S., Shin, H. H., Singh, G., Hubbell, B., and
862 Brauer, M.: An integrated risk function for estimating the global burden of disease attributable to ambient
863 fine particulate matter exposure, 2014.

864 Chipperfield, M. P.: New version of the TOMCAT/SLIMCAT off-line chemical transport model:
865 Intercomparison of stratospheric tracer experiments, Quarterly Journal of the Royal Meteorological Society,
866 132, 1179-1203, 10.1256/qj.05.51, 2006.

867 Chipperfield, M. P., Dhomse, S. S., Feng, W., McKenzie, R. L., Velders, G. J. M., and Pyle, J. A.: Quantifying the
868 ozone and ultraviolet benefits already achieved by the Montreal Protocol, Nat Commun, 6,
869 10.1038/ncomms8233, 2015.

870 Cofala, J., Amann, M., Klimont, Z., and Schopp, W.: Scenarios of World Anthropogenic Emissions of SO₂, NO_x
871 and CO up to 2030, International Institute for Applied Systems Analysis, Laxenburg, Austria, 2005.

872 Dentener, F., Kinne, S., Bond, T., Boucher, O., Cofala, J., Generoso, S., Ginoux, P., Gong, S., Hoelzemann, J. J.,
873 Ito, A., Marelli, L., Penner, J. E., Putaud, J. P., Textor, C., Schulz, M., van der Werf, G. R., and Wilson, J.:
874 Emissions of primary aerosol and precursor gases in the years 2000 and 1750 prescribed data-sets for
875 AeroCom, Atmos. Chem. Phys., 6, 4321-4344, 10.5194/acp-6-4321-2006, 2006.

876 Dessens, O., Köhler, M. O., Rogers, H. L., Jones, R. L., and Pyle, J. A.: Aviation and climate change, Transport
877 Policy, <http://dx.doi.org/10.1016/j.tranpol.2014.02.014>, 2014.

878 Dockery, D. W., Pope, C. A., Xu, X., Spengler, J. D., Ware, J. H., Fay, M. E., Ferris, B. G., and Speizer, F. E.: An
879 Association between Air Pollution and Mortality in Six U.S. Cities, New England Journal of Medicine, 329,
880 1753-1759, doi:10.1056/NEJM199312093292401, 1993.

881 DuBois, D., and Paynter, G. C.: "Fuel Flow Method2" for Estimating Aircraft Emissions, SAE Technical Paper
882 Series, 01, 2006.

883 Edwards, J. M., and Slingo, A.: Studies with a flexible new radiation code. I: Choosing a configuration for a
884 large-scale model, Quarterly Journal of the Royal Meteorological Society, 122, 689-719,
885 10.1002/qj.49712253107, 1996.

886 Eyers, C. J., Addleton, D., Atkinson, K., Broomhead, M. J., Christou, R., Elliff, T., Falk, R., Gee, I., Lee, D. S.,
887 Marizy, C., S Michot, Middel, J., Newton, P., Norman, P., Plohr, M., Raper, D., and Stanciou, N.: AERO2K
888 Global Aviation Emissions Inventories for 2002 and 2025, QINETIQ/04/01113, 2004.

889 Eyring, V., Isaksen, I. S. A., Berntsen, T., Collins, W. J., Corbett, J. J., Endresen, O., Grainger, R. G., Moldanova,
890 J., Schlager, H., and Stevenson, D. S.: Transport impacts on atmosphere and climate: Shipping, Atmospheric
891 Environment, 44, 4735-4771, <http://dx.doi.org/10.1016/j.atmosenv.2009.04.059>, 2010.

892 Fiore, A. M., Naik, V., Spracklen, D. V., Steiner, A., Unger, N., Prather, M., Bergmann, D., Cameron-Smith, P.
893 J., Cionni, I., Collins, W. J., Dalsoren, S., Eyring, V., Folberth, G. A., Ginoux, P., Horowitz, L. W., Josse, B.,
894 Lamarque, J.-F., MacKenzie, I. A., Nagashima, T., O'Connor, F. M., Righi, M., Rumbold, S. T., Shindell, D. T.,
895 Skeie, R. B., Sudo, K., Szopa, S., Takemura, T., and Zeng, G.: Global air quality and climate, Chemical Society
896 Reviews, 41, 6663-6683, 2012.

897 Fountoukis, C., and Nenes, A.: Continued development of a cloud droplet formation parameterization for
898 global climate models, Journal of Geophysical Research: Atmospheres, 110, D11212,
899 10.1029/2004JD005591, 2005.

900 Frömming, C., Ponater, M., Dahlmann, K., Grewe, V., Lee, D. S., and Sausen, R.: Aviation-induced radiative
901 forcing and surface temperature change in dependency of the emission altitude, J. Geophys. Res., 117,
902 D19104, 10.1029/2012JD018204, 2012.

903 Fuglestvedt, J., Berntsen, T., Myhre, G., Rypdal, K., and Skeie, R. B.: Climate forcing from the transport
904 sectors, *Proceedings of the National Academy of Sciences*, 105, 454-458, 10.1073/pnas.0702958104, 2008.

905 Gettelman, A., and Chen, C.: The climate impact of aviation aerosols, *Geophysical Research Letters*, 40, 2785-
906 2789, 10.1002/grl.50520, 2013.

907 Guenther, A., Hewitt, C. N., Erickson, D., Fall, R., Geron, C., Graedel, T., Harley, P., Klinger, L., Lerdau, M.,
908 McKay, W. A., Pierce, T., Scholes, B., Steinbrecher, R., Tallamraju, R., Taylor, J., and Zimmerman, P.: A global
909 model of natural volatile organic compound emissions, *Journal of Geophysical Research: Atmospheres*, 100,
910 8873-8892, 10.1029/94JD02950, 1995.

911 Halmer, M. M., Schmincke, H. U., and Graf, H. F.: The annual volcanic gas input into the atmosphere, in
912 particular into the stratosphere: a global data set for the past 100 years, *Journal of Volcanology and
913 Geothermal Research*, 115, 511-528, [http://dx.doi.org/10.1016/S0377-0273\(01\)00318-3](http://dx.doi.org/10.1016/S0377-0273(01)00318-3), 2002.

914 Hand, J. L., Schichtel, B. A., Malm, W. C., and Pitchford, M. L.: Particulate sulfate ion concentration and SO₂
915 emission trends in the United States from the early 1990s through 2010, *Atmos. Chem. Phys.*, 12, 10353-
916 10365, 10.5194/acp-12-10353-2012, 2012.

917 Heald, C. L., Coe, H., Jimenez, J. L., Weber, R. J., Bahreini, R., Middlebrook, A. M., Russell, L. M., Jolleys, M.,
918 Fu, T. M., Allan, J. D., Bower, K. N., Capes, G., Crosier, J., Morgan, W. T., Robinson, N. H., Williams, P. I.,
919 Cubison, M. J., DeCarlo, P. F., and Dunlea, E. J.: Exploring the vertical profile of atmospheric organic aerosol:
920 comparing 17 aircraft field campaigns with a global model, *Atmos. Chem. Phys.*, 11, 12673-12696,
921 10.5194/acp-11-12673-2011, 2011.

922 Hileman, J. I., and Stratton, R. W.: Alternative jet fuel feasibility, *Transport Policy*,
923 <http://dx.doi.org/10.1016/j.tranpol.2014.02.018>, 2014.

924 Holmes, C. D., Tang, Q., and Prather, M. J.: Uncertainties in climate assessment for the case of aviation NO_x,
925 *Proceedings of the National Academy of Sciences*, 108, 10997-11002, 10.1073/pnas.1101458108, 2011.

926 Hoor, P., Borken-Kleefeld, J., Caro, D., Dessens, O., Endresen, O., Gauss, M., Grewe, V., Hauglustaine, D.,
927 Isaksen, I. S. A., Jöckel, P., Lelieveld, J., Myhre, G., Meijer, E., Olivie, D., Prather, M., Schnadt Poberaj, C.,
928 Shine, K. P., Staehelin, J., Tang, Q., van Aardenne, J., van Velthoven, P., and Sausen, R.: The impact of traffic
929 emissions on atmospheric ozone and OH: results from QUANTIFY, *Atmos. Chem. Phys.*, 9, 3113-3136,
930 10.5194/acp-9-3113-2009, 2009.

931 Hopke, P. K.: *Receptor modeling in environmental chemistry*, v. 76, Wiley, 1985.

932 ICAO: Annual Report of the Council 2012, International Civil Aviation Organisation (ICAO), 2013.

933 Jacobson, M. Z., Wilkerson, J. T., Naiman, A. D., and Lele, S. K.: The effects of aircraft on climate and
934 pollution. Part II: 20-year impacts of exhaust from all commercial aircraft worldwide treated individually at
935 the subgrid scale, *Faraday Discussions*, 165, 369-382, 10.1039/C3FD00034F, 2013.

936 Kettle, A. J., and Andreae, M. O.: Flux of dimethylsulfide from the oceans: A comparison of updated data sets
937 and flux models, *Journal of Geophysical Research: Atmospheres*, 105, 26793-26808, 10.1029/2000JD900252,
938 2000.

939 Khodayari, A., Olsen, S. C., and Wuebbles, D. J.: Evaluation of aviation NO_x-induced radiative forcings for
940 2005 and 2050, *Atmospheric Environment*, 91, 95-103, <http://dx.doi.org/10.1016/j.atmosenv.2014.03.044>,
941 2014.

942 Knighton, W. B., Rogers, T. M., Anderson, B. E., Herndon, S. C., Yelvington, P. E., and Miake-Lye, R. C.:
943 Quantification of Aircraft Engine Hydrocarbon Emissions Using Proton Transfer Reaction Mass Spectrometry,
944 *Journal of Propulsion and Power*, 23, 949-958, 2007.

945 Köhler, M. O., Rädcl, G., Dessens, O., Shine, K. P., Rogers, H. L., Wild, O., and Pyle, J. A.: Impact of
946 perturbations to nitrogen oxide emissions from global aviation, *Journal of Geophysical Research:*
947 *Atmospheres*, 113, D11305, 10.1029/2007JD009140, 2008.

948 Köhler, M. O., Rädcl, G., Shine, K. P., Rogers, H. L., and Pyle, J. A.: Latitudinal variation of the effect of
949 aviation NO_x emissions on atmospheric ozone and methane and related climate metrics, *Atmospheric
950 Environment*, 64, 1-9, 10.1016/j.atmosenv.2012.09.013, 2013.

951 Konovalov, I. B., Beekmann, M., Burrows, J. P., and Richter, A.: Satellite measurement based estimates of
952 decadal changes in European nitrogen oxides emissions, *Atmos. Chem. Phys.*, 8, 2623-2641, 10.5194/acp-8-
953 2623-2008, 2008.

954 Lamarque, J. F., Hess, P., Emmons, L., Buja, L., Washington, W., and Granier, C.: Tropospheric ozone
955 evolution between 1890 and 1990, *Journal of Geophysical Research: Atmospheres*, 110, n/a-n/a,
956 10.1029/2004JD005537, 2005.

957 Lamarque, J. F., Bond, T. C., Eyring, V., Granier, C., Heil, A., Klimont, Z., Lee, D., Lioussse, C., Mieville, A., Owen,
 958 B., Schultz, M. G., Shindell, D., Smith, S. J., Stehfest, E., Van Aardenne, J., Cooper, O. R., Kainuma, M.,
 959 Mahowald, N., McConnell, J. R., Naik, V., Riahi, K., and van Vuuren, D. P.: Historical (1850–2000) gridded
 960 anthropogenic and biomass burning emissions of reactive gases and aerosols: methodology and application,
 961 *Atmos. Chem. Phys.*, 10, 7017–7039, 10.5194/acp-10-7017-2010, 2010.
 962 Lee, D. S., Fahey, D. W., Forster, P. M., Newton, P. J., Wit, R. C. N., Lim, L. L., Owen, B., and Sausen, R.:
 963 Aviation and global climate change in the 21st century, *Atmospheric Environment*, 43, 3520–3537,
 964 10.1016/j.atmosenv.2009.04.024, 2009.
 965 Lee, D. S., Pitari, G., Grewe, V., Gierens, K., Penner, J. E., Petzold, A., Prather, M. J., Schumann, U., Bais, A.,
 966 Berntsen, T., Iachetti, D., Lim, L. L., and Sausen, R.: Transport impacts on atmosphere and climate: Aviation,
 967 *Atmospheric Environment*, 44, 4678–4734, 10.1016/j.atmosenv.2009.06.005, 2010.
 968 Lim, S. S., Vos, T., Flaxman, A. D., Danaei, G., Shibuya, K., Adair-Rohani, H., AlMazroa, M. A., Amann, M.,
 969 Anderson, H. R., Andrews, K. G., Aryee, M., Atkinson, C., Bacchus, L. J., Bahalim, A. N., Balakrishnan, K.,
 970 Balmes, J., Barker-Collo, S., Baxter, A., Bell, M. L., Blore, J. D., Blyth, F., Bonner, C., Borges, G., Bourne, R.,
 971 Boussinesq, M., Brauer, M., Brooks, P., Bruce, N. G., Brunekreef, B., Bryan-Hancock, C., Bucello, C.,
 972 Buchbinder, R., Bull, F., Burnett, R. T., Byers, T. E., Calabria, B., Carapetis, J., Carnahan, E., Chafe, Z., Charlson,
 973 F., Chen, H., Chen, J. S., Cheng, A. T.-A., Child, J. C., Cohen, A., Colson, K. E., Cowie, B. C., Darby, S., Darling, S.,
 974 Davis, A., Degenhardt, L., Dentener, F., Des Jarlais, D. C., Devries, K., Dherani, M., Ding, E. L., Dorsey, E. R.,
 975 Driscoll, T., Edmond, K., Ali, S. E., Engell, R. E., Erwin, P. J., Fahimi, S., Falder, G., Farzadfar, F., Ferrari, A.,
 976 Finucane, M. M., Flaxman, S., Fowkes, F. G. R., Freedman, G., Freeman, M. K., Gakidou, E., Ghosh, S.,
 977 Giovannucci, E., Gmel, G., Graham, K., Grainger, R., Grant, B., Gunnell, D., Gutierrez, H. R., Hall, W., Hoek, H.
 978 W., Hogan, A., Hosgood Iii, H. D., Hoy, D., Hu, H., Hubbell, B. J., Hutchings, S. J., Ibeanusi, S. E., Jacklyn, G. L.,
 979 Jasrasaria, R., Jonas, J. B., Kan, H., Kanis, J. A., Kassebaum, N., Kawakami, N., Khang, Y.-H., Khatibzadeh, S.,
 980 Khoo, J.-P., Kok, C., Laden, F., Lalloo, R., Lan, Q., Lathlean, T., Leasher, J. L., Leigh, J., Li, Y., Lin, J. K., Lipshultz,
 981 S. E., London, S., Lozano, R., Lu, Y., Mak, J., Malekzadeh, R., Mallinger, L., Marcenes, W., March, L., Marks, R.,
 982 Martin, R., McGale, P., McGrath, J., Mehta, S., Memish, Z. A., Mensah, G. A., Merriman, T. R., Micha, R.,
 983 Michaud, C., Mishra, V., Hanafiah, K. M., Mokdad, A. A., Morawska, L., Mozaffarian, D., Murphy, T., Naghavi,
 984 M., Neal, B., Nelson, P. K., Nolla, J. M., Norman, R., Olives, C., Omer, S. B., Orchard, J., Osborne, R., Ostro, B.,
 985 Page, A., Pandey, K. D., Parry, C. D. H., Passmore, E., Patra, J., Pearce, N., Pelizzari, P. M., Petzold, M., Phillips,
 986 M. R., Pope, D., Pope III, C. A., Powles, J., Rao, M., Razavi, H., Rehfuess, E. A., Rehm, J. T., Ritz, B., Rivara, F. P.,
 987 Roberts, T., Robinson, C., Rodriguez-Portales, J. A., Romieu, I., Room, R., Rosenfeld, L. C., Roy, A., Rushton, L.,
 988 Salomon, J. A., Sampson, U., Sanchez-Riera, L., Sanman, E., Sapkota, A., Seedat, S., Shi, P., Shield, K.,
 989 Shivakoti, R., Singh, G. M., Sleet, D. A., Smith, E., Smith, K. R., Stapelberg, N. J. C., Steenland, K., Stöckl, H.,
 990 Stovner, L. J., Straif, K., Straney, L., Thurston, G. D., Tran, J. H., Van Dingenen, R., van Donkelaar, A., Veerman,
 991 J. L., Vijayakumar, L., Weintraub, R., Weissman, M. M., White, R. A., Whiteford, H., Wiersma, S. T., Wilkinson,
 992 J. D., Williams, H. C., Williams, W., Wilson, N., Woolf, A. D., Yip, P., Zielinski, J. M., Lopez, A. D., Murray, C. J.
 993 L., and Ezzati, M.: A comparative risk assessment of burden of disease and injury attributable to 67 risk
 994 factors and risk factor clusters in 21 regions, 1990–2010: a systematic analysis for the Global Burden of
 995 Disease Study 2010, *The Lancet*, 380, 2224–2260, [http://dx.doi.org/10.1016/S0140-6736\(12\)61766-8](http://dx.doi.org/10.1016/S0140-6736(12)61766-8), 2012.
 996 Mann, G. W., Carslaw, K. S., Spracklen, D. V., Ridley, D. A., Manktelow, P. T., Chipperfield, M. P., Pickering, S.
 997 J., and Johnson, C. E.: Description and evaluation of GLOMAP-mode: a modal global aerosol microphysics
 998 model for the UKCA composition-climate model, *Geosci. Model Dev.*, 3, 519–551, 10.5194/gmd-3-519-2010,
 999 2010.
 1000 Ministry of Defence: Defence Standard 91-91. Turbine Fuel, Kerosine Type, Jet A-1. NATO Code: F-35. Joint
 1001 Service Designation: AVTUR, Glasgow, United Kingdom, 2011.
 1002 Morita, H., Yang, S., Unger, N., and Kinney, P. L.: Global Health Impacts of Future Aviation Emissions Under
 1003 Alternative Control Scenarios, *Environmental Science & Technology*, 48, 14659–14667, 10.1021/es5055379,
 1004 2014.
 1005 Myhre, G., Shine, K. P., Rädel, G., Gauss, M., Isaksen, I. S. A., Tang, Q., Prather, M. J., Williams, J. E., van
 1006 Velthoven, P., Dessens, O., Koffi, B., Szopa, S., Hoor, P., Grewe, V., Borken-Kleefeld, J., Berntsen, T. K., and
 1007 Fuglestad, J. S.: Radiative forcing due to changes in ozone and methane caused by the transport sector,
 1008 *Atmospheric Environment*, 45, 387–394, 10.1016/j.atmosenv.2010.10.001, 2011.
 1009 Nenes, A., and Seinfeld, J. H.: Parameterization of cloud droplet formation in global climate models, *Journal*
 1010 *of Geophysical Research: Atmospheres*, 108, 4415, 10.1029/2002JD002911, 2003.

1011 Nightingale, P. D., Malin, G., Law, C. S., Watson, A. J., Liss, P. S., Liddicoat, M. I., Boutin, J., and Upstill-
 1012 Goddard, R. C.: In situ evaluation of air-sea gas exchange parameterizations using novel conservative and
 1013 volatile tracers, *Global Biogeochemical Cycles*, 14, 373-387, 10.1029/1999GB900091, 2000.
 1014 Olsen, S. C., Wuebbles, D. J., and Owen, B.: Comparison of global 3-D aviation emissions datasets, *Atmos.*
 1015 *Chem. Phys.*, 13, 429-441, 10.5194/acp-13-429-2013, 2013.
 1016 Ostro, B. D.: Outdoor air pollution: Assessing the environmental burden of disease at national and local
 1017 levels, 2004.
 1018 Pope, C. A., Burnett, R. T., Thun, M. J., Calle, E. E., Krewski, D., Ito, K., and Thurston, G. D.: Lung Cancer,
 1019 Cardiopulmonary Mortality, and Long-term Exposure to Fine Particulate Air Pollution, *JAMA*, 287, 1132-1141,
 1020 10.1001/jama.287.9.1132, 2002.
 1021 Pope, C. A., and Dockery, D. W.: Health effects of fine particulate air pollution: lines that connect, *Journal of*
 1022 *the Air & Waste Management Association*, 56, 709-742, 2006.
 1023 EU FP6 Integrated Project QUANTIFY. Quantifying the Climate Impact of Global and European Transport
 1024 Systems: QUANTIFY emission inventories and scenarios: <http://www.pa.op.dlr.de/quantify/>, access:
 1025 15/07/2011, 2005-2012.
 1026 Rap, A., Forster, P. M., Jones, A., Boucher, O., Haywood, J. M., Bellouin, N., and De Leon, R. R.:
 1027 Parameterization of contrails in the UK Met Office Climate Model, *J. Geophys. Res.*, 115, D10205,
 1028 10.1029/2009jd012443, 2010.
 1029 Rap, A., Scott, C. E., Spracklen, D. V., Bellouin, N., Forster, P. M., Carslaw, K. S., Schmidt, A., and Mann, G.:
 1030 Natural aerosol direct and indirect radiative effects, *Geophysical Research Letters*, 40, 3297-3301,
 1031 10.1002/grl.50441, 2013.
 1032 Rap, A., Richards, N. A. D., Forster, P. M., Monks, S. A., Arnold, S. R., and Chipperfield, M. P.: Satellite
 1033 constraint on the tropospheric ozone radiative effect, *Geophysical Research Letters*, 42, 2015GL064037,
 1034 10.1002/2015GL064037, 2015.
 1035 Ratliff, G., Sequeira, C., Waitz, I., Ohsfeldt, M., Thrasher, T., Graham, M., and Thompson, T.: Aircraft Impacts
 1036 on Local and Regional Air Quality in the United States, Massachusetts Institute of Technology PARTNER
 1037 report (Report No. PARTNER-COE-2009-002), 2009.
 1038 Richards, N. A. D., Arnold, S. R., Chipperfield, M. P., Miles, G., Rap, A., Siddans, R., Monks, S. A., and
 1039 Hollaway, M. J.: The Mediterranean summertime ozone maximum: global emission sensitivities and radiative
 1040 impacts, *Atmos. Chem. Phys.*, 13, 2331-2345, 10.5194/acp-13-2331-2013, 2013.
 1041 Righi, M., Hendricks, J., and Sausen, R.: The global impact of the transport sectors on atmospheric aerosol:
 1042 simulations for year 2000 emissions, *Atmos. Chem. Phys.*, 13, 9939-9970, 10.5194/acp-13-9939-2013, 2013.
 1043 Rossow, W. B., and Schiffer, R. A.: Advances in Understanding Clouds from ISCCP, *Bulletin of the American*
 1044 *Meteorological Society*, 80, 2261-2287, 10.1175/1520-0477(1999)080<2261:AIUCFI>2.0.CO;2, 1999.
 1045 Sausen, R., Isaksen, I., Grewe, V., Hauglustaine, D., Lee, D. S., Myhre, G., Köhler, M. O., Pitari, G., Schumann,
 1046 U., Stordal, F., and Zerefos, C.: Aviation radiative forcing in 2000: An update on IPCC (1999), *Meteorologische*
 1047 *Zeitschrift*, 14, 555-561, 2005.
 1048 Schmidt, A., Carslaw, K. S., Mann, G. W., Rap, A., Pringle, K. J., Spracklen, D. V., Wilson, M., and Forster, P.
 1049 M.: Importance of tropospheric volcanic aerosol for indirect radiative forcing of climate, *Atmos. Chem. Phys.*,
 1050 12, 7321-7339, 10.5194/acp-12-7321-2012, 2012.
 1051 Skowron, A., Lee, D. S., and De León, R. R.: The assessment of the impact of aviation NO_x on ozone and other
 1052 radiative forcing responses – The importance of representing cruise altitudes accurately, *Atmospheric*
 1053 *Environment*, 74, 159-168, <http://dx.doi.org/10.1016/j.atmosenv.2013.03.034>, 2013.
 1054 Spicer, C. W., Holdren, M. W., Riggin, R. M., and Lyon, T. F.: Chemical composition and photochemical
 1055 reactivity of exhaust from aircraft turbine engines, *Ann. Geophys.*, 12, 944-955, 10.1007/s00585-994-0944-0,
 1056 1994.
 1057 Spracklen, D. V., Pringle, K. J., Carslaw, K. S., Chipperfield, M. P., and Mann, G. W.: A global off-line model of
 1058 size-resolved aerosol microphysics: I. Model development and prediction of aerosol properties, *Atmospheric*
 1059 *Chemistry and Physics*, 5, 2227-2252, 2005.
 1060 Spracklen, D. V., Carslaw, K. S., Merikanto, J., Mann, G. W., Reddington, C. L., Pickering, S., Ogren, J. A.,
 1061 Andrews, E., Baltensperger, U., Weingartner, E., Boy, M., Kulmala, M., Laakso, L., Lihavainen, H., Kivekäs, N.,
 1062 Komppula, M., Mihalopoulos, N., Kouvarakis, G., Jennings, S. G., O'Dowd, C., Birmili, W., Wiedensohler, A.,
 1063 Weller, R., Gras, J., Laj, P., Sellegri, K., Bonn, B., Krejci, R., Laaksonen, A., Hamed, A., Minikin, A., Harrison, R.

1064 M., Talbot, R., and Sun, J.: Explaining global surface aerosol number concentrations in terms of primary
 1065 emissions and particle formation, *Atmos. Chem. Phys.*, 10, 4775-4793, 10.5194/acp-10-4775-2010, 2010.
 1066 Spracklen, D. V., Carslaw, K. S., Pöschl, U., Rap, A., and Forster, P. M.: Global cloud condensation nuclei
 1067 influenced by carbonaceous combustion aerosol, *Atmos. Chem. Phys.*, 11, 9067-9087, 10.5194/acp-11-9067-
 1068 2011, 2011a.
 1069 Spracklen, D. V., Jimenez, J. L., Carslaw, K. S., Worsnop, D. R., Evans, M. J., Mann, G. W., Zhang, Q.,
 1070 Canagaratna, M. R., Allan, J., Coe, H., McFiggans, G., Rap, A., and Forster, P.: Aerosol mass spectrometer
 1071 constraint on the global secondary organic aerosol budget, *Atmos. Chem. Phys.*, 11, 12109-12136,
 1072 10.5194/acp-11-12109-2011, 2011b.
 1073 Stevenson, D. S., and Derwent, R. G.: Does the location of aircraft nitrogen oxide emissions affect their
 1074 climate impact?, *Geophysical Research Letters*, 36, L17810, 10.1029/2009GL039422, 2009.
 1075 Stevenson, D. S., Young, P. J., Naik, V., Lamarque, J. F., Shindell, D. T., Voulgarakis, A., Skeie, R. B., Dalsoren,
 1076 S. B., Myhre, G., Berntsen, T. K., Folberth, G. A., Rumbold, S. T., Collins, W. J., MacKenzie, I. A., Doherty, R.
 1077 M., Zeng, G., van Noije, T. P. C., Strunk, A., Bergmann, D., Cameron-Smith, P., Plummer, D. A., Strode, S. A.,
 1078 Horowitz, L., Lee, Y. H., Szopa, S., Sudo, K., Nagashima, T., Josse, B., Cionni, I., Righi, M., Eyring, V., Conley, A.,
 1079 Bowman, K. W., Wild, O., and Archibald, A.: Tropospheric ozone changes, radiative forcing and attribution to
 1080 emissions in the Atmospheric Chemistry and Climate Model Intercomparison Project (ACCMIP), *Atmos.*
 1081 *Chem. Phys.*, 13, 3063-3085, 10.5194/acp-13-3063-2013, 2013.
 1082 Thompson, A. M., Tao, W.-K., Pickering, K. E., Scala, J. R., and Simpson, J.: Tropical Deep Convection and
 1083 Ozone Formation, *Bulletin of the American Meteorological Society*, 78, 1043-1054, 10.1175/1520-
 1084 0477(1997)078<1043:TDCOAF>2.0.CO;2, 1997.
 1085 Tilmes, S., Lamarque, J. F., Emmons, L. K., Conley, A., Schultz, M. G., Saunio, M., Thouret, V., Thompson, A.
 1086 M., Oltmans, S. J., Johnson, B., and Tarasick, D.: Technical Note: Ozone sonde climatology between 1995 and
 1087 2011: description, evaluation and applications, *Atmos. Chem. Phys.*, 12, 7475-7497, 10.5194/acp-12-7475-
 1088 2012, 2012.
 1089 Uherek, E., Halenka, T., Borken-Kleefeld, J., Balkanski, Y., Berntsen, T., Borrego, C., Gauss, M., Hoor, P., Juda-
 1090 Rezler, K., Lelieveld, J., Melas, D., Rypdal, K., and Schmid, S.: Transport impacts on atmosphere and climate:
 1091 Land transport, *Atmospheric Environment*, 44, 4772-4816,
 1092 <http://dx.doi.org/10.1016/j.atmosenv.2010.01.002>, 2010.
 1093 Unger, N., Shindell, D. T., Koch, D. M., and Streets, D. G.: Cross influences of ozone and sulfate precursor
 1094 emissions changes on air quality and climate, *Proceedings of the National Academy of Sciences of the United*
 1095 *States of America*, 103, 4377-4380, 10.1073/pnas.0508769103, 2006.
 1096 Unger, N.: Global climate impact of civil aviation for standard and desulfurized jet fuel, *Geophys. Res. Lett.*,
 1097 38, L20803, 10.1029/2011gl049289, 2011.
 1098 Unger, N., Zhao, Y., and Dang, H.: Mid-21st century chemical forcing of climate by the civil aviation sector,
 1099 *Geophysical Research Letters*, 40, 641-645, 10.1002/grl.50161, 2013.
 1100 Van Der Werf, G. R., Randerson, J. T., Collatz, G. J., and Giglio, L.: Carbon emissions from fires in tropical and
 1101 subtropical ecosystems, *Global Change Biology*, 9, 547-562, 10.1046/j.1365-2486.2003.00604.x, 2003.
 1102 van der Werf, G. R., Randerson, J. T., Giglio, L., Collatz, G. J., Mu, M., Kasibhatla, P. S., Morton, D. C., DeFries,
 1103 R. S., Jin, Y., and van Leeuwen, T. T.: Global fire emissions and the contribution of deforestation, savanna,
 1104 forest, agricultural, and peat fires (1997–2009), *Atmos. Chem. Phys.*, 10, 11707-11735, 10.5194/acp-10-
 1105 11707-2010, 2010.
 1106 Vestreng, V., Myhre, G., Fagerli, H., Reis, S., and Tarrasón, L.: Twenty-five years of continuous sulphur dioxide
 1107 emission reduction in Europe, *Atmos. Chem. Phys.*, 7, 3663-3681, 10.5194/acp-7-3663-2007, 2007.
 1108 Wayson, R. L., Fleming, G. G., and Iovinelli, R.: Methodology to Estimate Particulate Matter Emissions from
 1109 Certified Commercial Aircraft Engines, *Journal of the Air & Waste Management Association*, 59, 91-100,
 1110 10.3155/1047-3289.59.1.91, 2009.
 1111 Whitburn, S., Van Damme, M., Kaiser, J. W., van der Werf, G. R., Turquety, S., Hurtmans, D., Clarisse, L.,
 1112 Clerbaux, C., and Coheur, P. F.: Ammonia emissions in tropical biomass burning regions: Comparison
 1113 between satellite-derived emissions and bottom-up fire inventories, *Atmospheric Environment*,
 1114 <http://dx.doi.org/10.1016/j.atmosenv.2015.03.015>, 2015.
 1115 Wilkerson, J. T., Jacobson, M. Z., Malwitz, A., Balasubramanian, S., Wayson, R., Fleming, G., Naiman, A. D.,
 1116 and Lele, S. K.: Analysis of emission data from global commercial aviation: 2004 and 2006, *Atmos. Chem.*
 1117 *Phys.*, 10, 6391-6408, 10.5194/acp-10-6391-2010, 2010.

1118 Woody, M., Haeng Baek, B., Adelman, Z., Omary, M., Fat Lam, Y., Jason West, J., and Arunachalam, S.: An
1119 assessment of Aviation's contribution to current and future fine particulate matter in the United States,
1120 Atmospheric Environment, 45, 3424-3433, 10.1016/j.atmosenv.2011.03.041, 2011.
1121 World Health Organisation: Health Aspects of Air Pollution with Particulate Matter, Ozone and Nitrogen
1122 Dioxide, Bonn, Germany, 2003.
1123 World Health Organisation: Air Quality Guidelines a Global Update 2005: Particulate matter, ozone, nitrogen
1124 dioxide and sulphur dioxide, Germany, 2005.
1125 Yim, N.-H., Kim, S.-H., Kim, H.-W., and Kwahk, K.-Y.: Knowledge based decision making on higher level
1126 strategic concerns: system dynamics approach, Expert Systems with Applications, 27, 143-158, DOI:
1127 10.1016/j.eswa.2003.12.019, 2004.
1128 Yim, S. H. L., Lee, G. L., Lee, I. H., Allroggen, F., Ashok, A., Caiazzo, F., Eastham, S. D., Malina, R., and Barrett,
1129 S. R. H.: Global, regional and local health impacts of civil aviation emissions, Environmental Research Letters,
1130 10, 034001, 2015.
1131 Young, P. J., Archibald, A. T., Bowman, K. W., Lamarque, J. F., Naik, V., Stevenson, D. S., Tilmes, S.,
1132 Voulgarakis, A., Wild, O., Bergmann, D., Cameron-Smith, P., Cionni, I., Collins, W. J., Dalsøren, S. B., Doherty,
1133 R. M., Eyring, V., Faluvegi, G., Horowitz, L. W., Josse, B., Lee, Y. H., MacKenzie, I. A., Nagashima, T., Plummer,
1134 D. A., Righi, M., Rumbold, S. T., Skeie, R. B., Shindell, D. T., Strode, S. A., Sudo, K., Szopa, S., and Zeng, G.: Pre-
1135 industrial to end 21st century projections of tropospheric ozone from the Atmospheric Chemistry and
1136 Climate Model Intercomparison Project (ACCMIP), Atmos. Chem. Phys., 13, 2063-2090, 10.5194/acp-13-
1137 2063-2013, 2013.
1138
1139
1140
1141
1142
1143
1144
1145
1146
1147
1148
1149
1150
1151
1152
1153
1154
1155
1156
1157
1158
1159
1160
1161
1162
1163
1164
1165
1166
1167
1168
1169
1170
1171